Construction of Taiwanese Brain Template from MR Images

A thesis presented

by

Ying-Ying Chao

to

Institute of Computer Science and Engineering

College of Computer Science
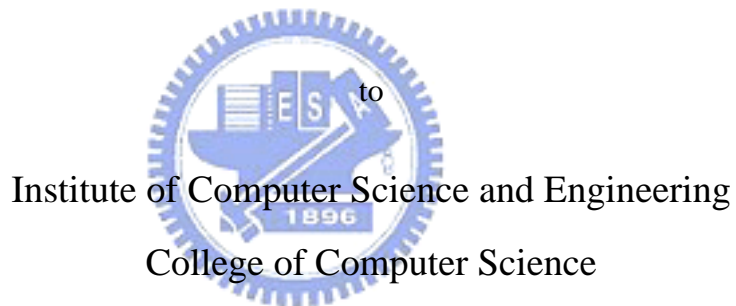
in partial fulfillment of the requirements

for the degree of

Master

in the subject of

Computer Science

National Chiao Tung University

Hsinchu, Taiwan

2006

Construction of Taiwanese Brain Template

from MR Images

Copyright © 2006

by

Ying-Ying Chao

Abstract

Brain template is essential to functional and structural brain mapping. It provides a standard stereotaxic space containing a set of anatomical and functional labels annotated at specific coordinates. An individual brain can be spatially normalized into this standard space to incorporate the annotation information. Furthermore, only in this same space that brain MR images can be compared to obtain statistical inference of structural discrepancy. MNI305 is a widely-used brain template, which was created by Montreal Neurological Institute from 305 brain MRI volumes of Western normal subjects. However, inter-ethnic difference of brain structure can be large. Normalizing the brain to a template of different race may cause structural artefact due to the large spatial distortion. Therefore, a customized brain template is necessary for structural brain analysis for Easter people.
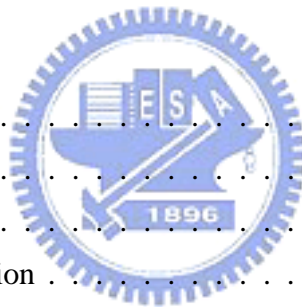
In this work, we develop associated algorithms and construct a Taiwanese brain template from a database containing brain MRI volumes of Taiwanese for both genders. First, we propose an estimation technique that can automatically determine the mid-sagittal plane for each individual MRI. Then, the anatomical landmark, anterior commissure (AC), is selected as the origin point and another anatomical landmark, posterior commissure (PC), is selected such that the AC-PC line constitutes the mapping axis. We choose an individual MRI as the representative brain and register all other MRIs to the same stereotaxic coordinate space by aligning their mid-sagittal planes, origins, and mapping axes to those of the representative brain. Finally, the brain template is obtained by averaging all of the spatially normalized brain MRIs.

In this study, we also demonstrate that the constructed Taiwanese brain template can be used to reduce the amount of spatial normalization distortion when Taiwanese brain MRIs are involved in structural analysis. Another finding shows that Taiwanese brain template is shorter and wider than Western templates.

Contents

List of Figures

List of Tables

Chapter 1

Introduction

1.1 Backgrounds

Magnetic resonance imaging (MRI) is a modern technology in 21th century. It is a visualization method used to observe inner side of living organisms without physically breaking the outside tissue. Therefore, it becomes a widely used technology on medical diagnosis and pathological studies.

There are many advantages of MR technology. Aside from MRI system uses a non-invasive method to examine the organisms inside a living body. There is no reported injury which is caused by MRI scanner after scanning until now. Otherwise, MR image is high resolution and could provide the inner soft tissue from any direction. An disadvantage of MR system is that the device is so expansive, approximately costs one million US dollar per tesla for each unit, and also costs hundred thousand dollars per year to maintain.

For the importance of MRI, the Nobel Prize in Physiology or Medicine has jointed awarded to Paul Lauterbur and Peter Mansfield, the first member of discoverers on MRI, for their contribution on magnetic resonance imaging (MRI) system. Professor Lauterbur discovered MRI technology in 1973 by accident. He was an assistant professor in State University of New York at that time. One day he whimsically added the magnetic field gradients to the normally homogeneous main magnetic field, which used to produce nuclear magnetic resonance (NMR) signal. Surprisingly, the results allowed the spatial resolution instead of spectral resolution in general. Professor Lauterbur has send this discovery in Nature [22]. However, it was rejected. Although this work was rejected by Nature at that time, Peter Mansfield later recognized this discovery could be used to directly provide spatial information. Combining this discovery with the echo-planar imaging technique, which is also developed by Mansfield, MRI system now could rapidly display the scanning images at once.

Since the contribution of magnetic resonance imaging system made by Paul C. Lauter-
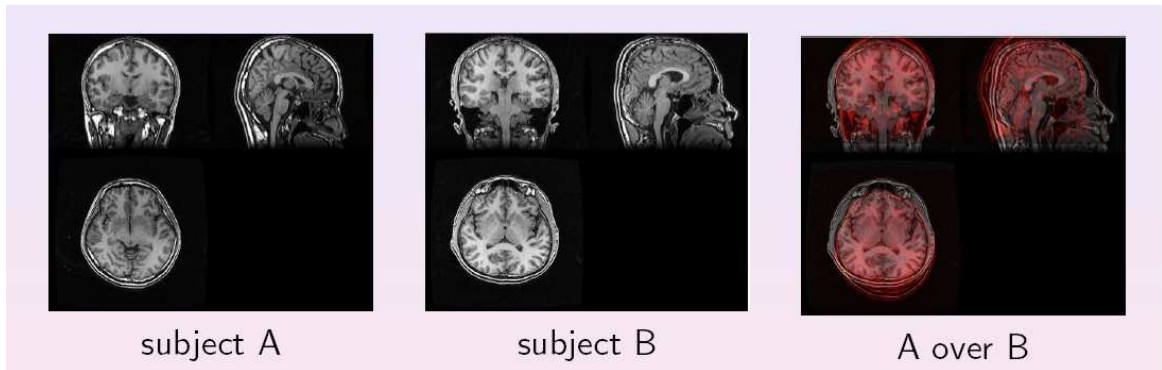
Figure 1.1: **Diversities of brain volumes.** (left) Subject A's brain MRI volume. (middle) Subjects B's brain MRI volume. (right) Overlap subject A's head onto subject B's head. Since brain shape, brain size and the scanning pose vary from person to person. We can not simply pick the same voxel in order to compare the difference between different brain MRI volumes.

bur and Peter Mansfield, this development accelerate the presence of modern magnetic resonance scanner. Nowadays, using 3D stereo volume which constructed by the scanner to assist doctors diagnosing is really a common way. It is a turning point of the medical diagnosis and routine inspection. Consequently, there are more and more researches focus on these MRI volumes. For instances, with the progress of the quality in medical images, Greitz, Bohm, Holte, and Eriksson [11] have developed a 3D digital atlas of the human brain by computerized 3D visualization technology.

In many brain diagnostic and its related works, the relationship of the brain structure between different subjects is necessary to be known. However, there is no reason to quite simply compare the same position voxel in different volume because of the non-equivalent brain shape and size. Otherwise, even the same tester, their brain do not lay the same orientation and position on the MRI machine. Therefore, the same position voxel in different volume clearly do not hold the same brain structure. As the reasons said above, a standard 3D brain structure space, said a brain template, is needed to convince the correctness and soundness of all these related brain studies.

Once we have a standard 3D brain structure space, we normalize different MR volumes to the standard space to compare the difference between them. Nevertheless, normalization lead to volume deformation. That is, if we do the rotation and scaling on MR volume in order to map onto the standard space, the cost we have to pay is the inaccuracy of the transformed volume. For the researchers, the less the distortion, the more reliability of the study. In other words, we must choose the brain template with exceptional caution.

Talairach brain is a commonly used brain template. It was a French woman's brain which anatomized by Talairach and Tournoux [37]. On the other hand, Evans, Collins, Mills, Brown, Kelly, and Peters [7] in Montreal Neurological Institute (MNI) constructed a standard brain template by 305 western young men who have normally functional brain. These two brain templates are regularly chose by related researchers. However, we may figure out that the brain size of western people is larger than the brain size of eastern people by the observation that the western people generally have bigger bodies.

As a matter of fact, according to Zilles, Kawashima, Dabringhaus, Fukuda, and Schormann [43], they indeed claim that there is inter-ethnic difference of brain structure. The Japanese brains are shorter, wider than the European brains. Thus, if we normalize the Taiwanese brain to the standard brain template which constructed primarily from the western population, the inaccuracy is apparently larger than normalize to the template constructed primarily from eastern people. In order to reduce the inaccuracy, we collect lots of Taiwanese brain subjects which come from both age and gender groups in order to create a brain template which is more suitable to the Taiwanese brains. The resulting Taiwanese brain template will improve the accuracy of structural brain studies when Taiwanese people are involved.

For another practical use, the Taiwanese brain template could be a bridge between Talairach Brain and individual brain. Talairach Brain is a specific brain which connected to Brodmann map as well as the Brodmann map is foundation of brain functional region. Once the Taiwanese brain template is constructed, the transformation relationship between

these two brain templates could be determined. Thus, whatever given functional brain structure images or a brain electrical activation signal map, the researchers could recognize the activation area of Brodmann area.

1.2 Related Works

Brodmann Map

Brodmann map is a map which defined the cerebral cortex by its cellular anatomy. This work was done by a German neurologist, Koribian Brodmann(1868-1918), in 1909. Brodmann structured several normal human brains under microscope to separate cerebral cortex into 52 anatomic regions, called the Brodmann areas, which he judged to be anatomically independent. It was conjectured that the neuron belong to the same cellular organization may work for the same function. From then on, quantities of researches were progressed based on Brodmann map. Until now, there are lots of studies that indicate the corresponding relationship between human brain function and Brodmann areas. For example, function of primary vision is about the Brodmann area 17 and of primary motor is about the Brodmann area 4. Although Brodmann map was drawn up about a century ago and is nowadays somewhat insufficient for detailed functional brain imaging, it is still a popular cyto-architectonic map used in cognitive neuroscience.

Talairach Brain

In 1988, Talairach and Tournoux [37] labeled Brodmann map onto their stereotaxic atlas, which called Talairach brain. They dissected an old French female's brain and photographed every slices then labeled the region of the Brodmann area. They also defined a standard coordinate system based on Talairach brain. Nowadays Talairach coordinate has
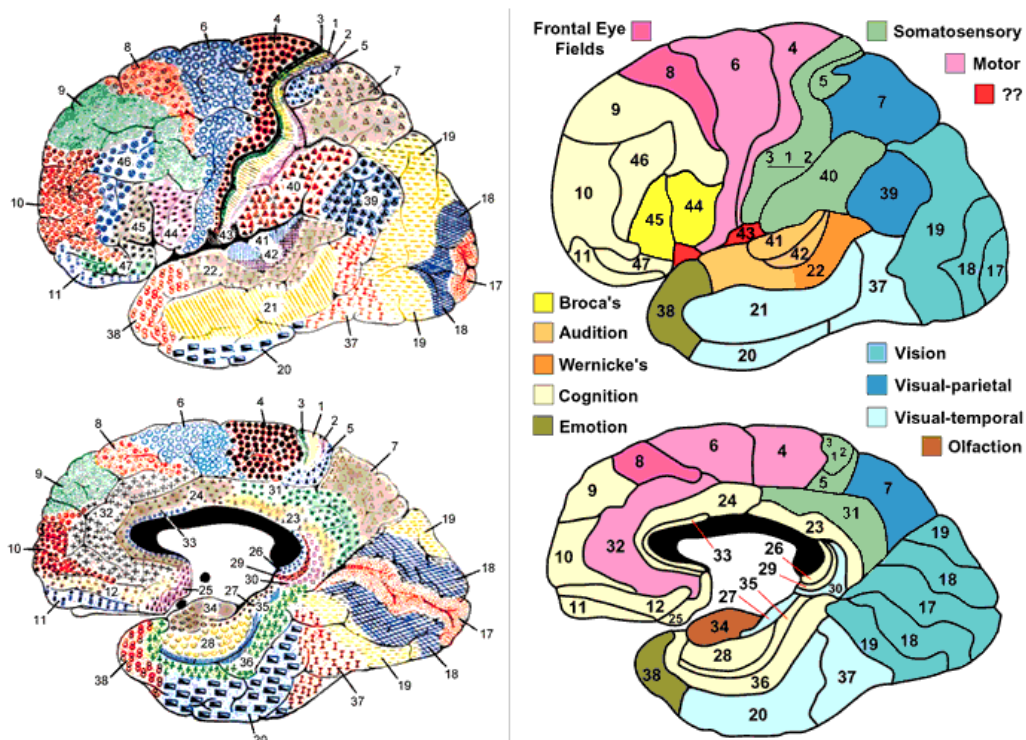
Figure 1.2: **Brodmann map.** Brodmann map was defined by cyto-architectonic method in 1909. It was divided into 52 distinct regions which was called Brodmann areas. A Brodmann area was considered as a cellular organization which may active for the same function. From then on, lots of studies have confirmed the relationship between Brodmann map and human brain functional areas.
(Graphic source : http://spot.colorado.edu/ dubin/talks/brodmann/brodmann.html)

became a commonly used stereotaxic space. Talairach brain makes it possible to obtain the related Brodmann area from the position of the Talairach coordinate. In other words, if we put a brain volume in Talairach coordinate, we could figure out the proper function of any region in brain.

However, even Talairach brain could map with the Brodmann area, some disadvantages still exist. First, a 60-year-old French woman definitely could not stand as the representative brain of most people. Second, there was an irrational assumption of the Talairach brain. Talairach and Tournoux [37] had assumed that the human brain is perfectly symmetry. It is

no doubt that this assumption is ridiculous. The last, thickness of slices is 4mm. It is too large the spatial interval that we certainly can not recover a whole brain from these slices.

MNI305

In 1994, Evans, Collins, Mills, Brown, Kelly, and Peters [7] in MNI tempted to set up a brain structure space which is more representative of the population. They select 305 normal subjects to construct a standard brain template which approximate the Talairach brain. This brain template is called MNI305. MNI305 was built by a two-stage method. First, 241 normal MRI volumes were took to fit the Talairach atlas. They manually picked several landmarks on each of these 241 brain volumes in order to determine an origin, said the anterior commissure (AC), and a reference line, said AC-PC line which passed AC and the posterior commissure (PC). Then they defined three orthogonal axes and finally fit these 241 brain volumes to the target volume, Talairach brain, by a 9 parameter linear transformation. In the second stage, 305 normal MRI volumes were took to be processed as the same procedure in the first stage. The only difference between these two stages is that the average of the transformed 241 brain volumes in stage one substitute as the target volume in stage two. The purpose of the second stage is to reduce the subjectivity of manually selection of the landmarks. Finally, they got an average MRI volume which nowadays named as MNI305. MNI305 is the first template constructed by MNI.

ICBM152 and ICBM452

Consequently, International Consortium for Brain Mapping (ICBM) adopted MNI305 as their standard template and used 152 normal subjects brain MR scans which normalized to MNI305 with 9 parameter affine transformation to construct another brain template, which is called ICBM152[28]. According to the official website of ICBM (http://www.loni.ucla.edu/ICBM), the newest ICBM brain template was constructed by 452

normal young adults brains.

Colin27

A member of MNI, Colin Holmes, had scanned 27 times for T1-weighted volume data. These data were in high resolution and came from the same person. Holmes, Hoge, Collins, Woods, Toga, and Evans [14] then register these 27 volumes together to create an average brain, which called Colin27. The resulting template, Colin27, had a high quality of signal-to-noise ratio (SNR). Therefore, these clear images could be useful for brain structure definition and any other anatomical studies.

Japanese Brain

In Asia, Sato, Taki, Fukuda, and Kawashima [31] collected 1547 normal and right-handed Japanese adults MR volumes, including 772 men, 775 women and the age range is between 16 to 79. They separated these subjects into groups according to the age. Then, a reference brain was selected from each group. By normalizing every individual brain subject to the reference brain of its age group, the measurement of age-related structural variation was detected.

Korean Template

78 normal and right-handed scanned MR and PET brain volumes was collected by Lee et al. [23]. These subjects were divided into groups of gender and groups of age (youth and elder). Two target brains were selected for gender group by semi-auto selection method. All brain subjects were normalized to the target brain of its gender group. Finally, four templates of youth men, elder men, youth women and elder women were constructed.

On the other way, 100 healthy Koreans (age : 39 ± 17 years old, M/F = 53/47) were collected to form a Korean template [18]. In Kim et al. [18]'s study, they compared the difference between Korean template and some other Western templates. A conclusion was that Korean brain volumes are wider, shorter and smaller than Western people's.

1.3   Thesis Scope

In this thesis, it is our attempt to construct a brain template. The intuition to build a template is to average all brain volumes and let the resulting average brain be the template. However, due to the impact of the brain shape, brain size and the diversity of the scanning position, the average brain is definitely too blurred to offer any information. Thus, we shall define a mapping plane, a mapping line and a mapping point in order to register different brains together. By referring to the Talairach coordinate, the mapping plane would be the mid-sagittal plane (MSP), the mapping line would be the line passing through anterior commissure (AC) and posterior commissure (PC), and the mapping point would be AC. After we fit all these features together, the remaining things are simply scaling and averaging.

We could separate the procedure of our template construction into two parts. The first part tells the estimation of mid-sagittal plane (MSP). The second part illustrates the major steps of construction, including the determination of the representative brain, head registration method and finally the averaging.

Inputing a volume data which is T1 images, we first process it by our auto-estimation MSP program and output a MSP-corrected volume data. The experts will check T1, T2 and PD images to see if the volume data is a normal brain. The abnormal brains would be exclude. Then the experts will examine if the auto-estimated MSP is perfect enough. If not, the experts would manually correct it. If it does good, this brain volume passes the test of experts. Finally, the experts would select several landmarks on these passed brain volumes
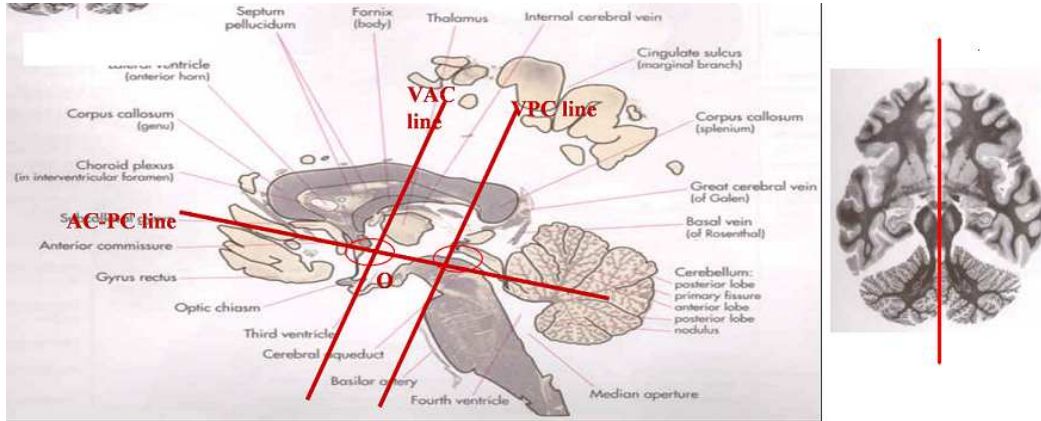
Figure 1.3: **Features for mapping individual brains to template.** In order to register the brain volume reasonably, we should take a representative soft tissue as the mapping feature. According to the Talairach coordinate, we select anterior commissure (AC) as the mapping point, the line passing through ac and posterior commissure (PC), said AC-PC line, as the mapping line, and the mid-sagittal plane (MSP) as the mapping plane. (left) This figure shows AC-PC line and two commissure AC (the left intersection point) and PC (the right intersection point). (right) MSP is what we called the inter-hemispheric (longitudinal) fissure which approximately bisect human brain into bilateral symmetry. This figure shows MSP on axial view.

for the use of following steps.

To begin with brain registration procedure, we need to select a representative brain from these brain volumes and then transform representative brain's AC and PC onto all the other brain volumes. The transformed AC and PC are denoted as AC_R and PC_R. These two transformed landmarks, AC_R and PC_R, jointly play a major role on brain registration. AC_R was set as the mapping origin, and AC_R-PC_R line was set as the mapping line. As the result, we orientate the AC_R-PC_R line to horizon and align AC_R on the same point. At this moment could we do the scaling. The size of every brain volume would scale to the size of representative brain. In the end, brain template is constructed by averaging these processed volumes.

In brief, our brain template construction method can be described as the following steps. For each subjects,
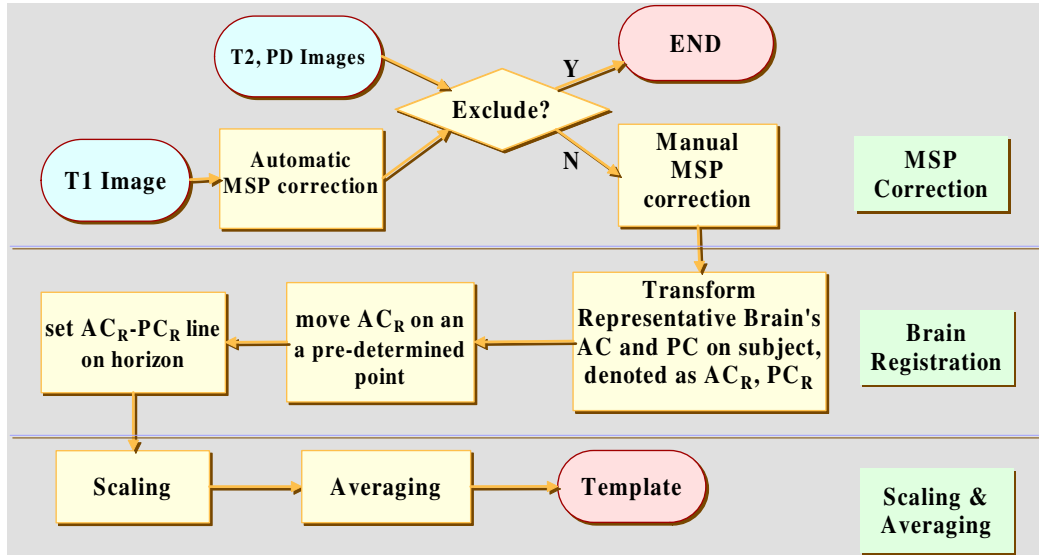
Figure 1.4: **Flow chart of template construction.** This figure describes the processed flow chart of an input brain volume. The first part is MSP correction. In this part, volume data would be examined by the experts to see if it is normal. If not, we will exclude this brain volume out of our experiment. If it is a normal brain, the experts would check if the estimation of MSP is good enough. If not, the experts would manually correct to a more precise one. At the end of this step, the experts will select several landmarks for the use of following steps. At the second part, we transform the representative brain's AC and PC onto the input volume data. The following steps are to put the transformed AC on a predetermined point and orientate the transformed AC-PC line horizontal for the purpose of alignment. Finally, the third part is to scale the input volume to the size of representative brain. In the end, we average all brain volumes to obtain the brain template.

1. Estimation of MSP

2. Selection of representative brain

3. Determination of AC point and AC-PC line

4. Alignment of AC point and AC-PC line

5. Scaling

In the end, we average all subjects and smooth the averaging image.

1.4   Thesis Organization

In the following chapters, we will present our algorithm, experiment results, and finally the discussion. In chapter 2 and chapter 3, we bring up our idea of template construction. Chapter 2 "Estimation of Mid-sagittal Plane" could be regarded as the necessary pre-processing step when comparing the brain structures. Only if we know the location of MSP, we can align different brain volumes together and do the other processing steps. In chapter 3, we show the construction steps in order. In chapter 4, we take experiments on our method. Finally in chapter 5 and 6, we have a discussion and conclusion.

Chapter 2

Estimation of Mid-sagittal Plane

2.1   Introduction

The interhemispheric (longitudinal) fissure approximately bisect human brain to bilateral symmetry. This symmetry plane is called mid-sagittal plane (MSP). MSP is a critical feature while referring to the Talairach coordinate. There is no doubt that estimation of MSP is usually the essential preprocess of brain registration, for it is reasonable to map everyone's MSP together. In addition, it is also the key factor of brain normalization, brain segmentation, tumor detection[27] and landmarks detection[17]. Obviously, identifying the MSP is of great assistance in pathology and clinical diagnosis. However, we should keep in mind that normal brains are usually asymmetry and MSP always forms a curved surface instead of a flat plane[36]. For these reasons, no explicit statement of MSP was defined in medical science.

2.2   Previous Works

Several approaches have been proposed to estimate MSP on MRI. Liu, Collins, and Rothfus [24, 25] tried to detect yaw angle on each axial slices. After this step, they approximate roll angle based on these detected yaw angles and thus extract a MSP. Consequently, Mykkänen et al. [29] have extended this method on PET images. Prima et al. [30] used an iterative two-stage scheme. The first stage is block matching method in order to obtain the displacement field. The second stage is to estimate a MSP by least trimmed squares (LTS) method. The procedure would be iterative processed until it goes into the converged condition. Teverovskiy and Liu [38] consider only the planes which close to centroid and embedded lattices from coarse to fine on a unit sphere in order to calculate each node. This calculation tries to give scores of each candidate MSP. Finally, they picked a MSP which got the highest score. Hu and Nowinski [15] tried to locate fissure line segments on every axial slices. Then they calculate the orientation and translation of final position of the fis-

sure line in each slices. In the end, by excluding the outliers of the these line segments, they used least-square method to approximate MSP. Ardekani et al. [2], Tuzikov et al. [39, 40] and Stegmann et al. [36] used simplex optimization method to approximate a precise MSP from each iteration to iteration. Dealing with optimization method, avoid falling into local minimum is what needs to put into consideration. And the solution is about the initial values and the objective function.

2.3   Proposed Method of Mid-sagittal Plane Estimation
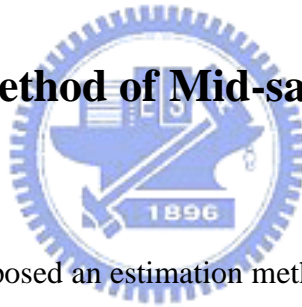
In this section, we proposed an estimation method for mid-sagittal plane. The input of this estimation model is the brain volume provided by the hospital and the output would be the input brain volume with its MSP transformed as the mid-line plane. Inside this estimation model, simplex optimization method is used to extract MSP.

There are two criteria we used to measure how good a MSP represented. The first criterion is that MSP could separate the brain as symmetry as possible. Cross-correlation value was calculated about the corresponding voxels of left hemisphere and right hemisphere. The second criterion is that an ideal MSP should contain no cortex on it. Because an ideal MSP could separate left hemisphere and right hemisphere as clearly as possible, just as Talairach Brain shows. For this criterion, we first selected a region of interest (ROI) upon the estimated MSP and then summed up the voxel intensity inside ROI. Regards to these two criteria, the higher the cross-correlation value as well as the lower the summation of intensity is what we expected.

2.3.1   Estimation Model

Input : Volume Data Coordinate C_O

Given a volume data $\mathbf{V}$, we say that this volume is in its volume data coordinate C_O. The origin in C_O is set on the left bottom corner of the volume data. Besides, the axes are denoted as $\mathbf{x_O}$, $\mathbf{y_O}$ and $\mathbf{z_O}$. Under the volume data coordinate C_O, MSP F is represented as

$$F = \mathbf{n} \cdot \begin{bmatrix} x \\ y \\ z \end{bmatrix} = \mathbf{n} \cdot \mathbf{m_C} + t, \tag{2.1}$$

where $(x,y,z) \in \mathbf{V}$. Let MSP origin $\mathbf{o_M}$ be the projection of mass center $\mathbf{m_C}$ on MSP F, and t is the distance from $\mathbf{m_C}$ to $\mathbf{o_M}$ where $\mathbf{n}$ is the plane normal unit vector.

Output : MSP coordinate C_M

It is our intension that the MSP could be in the middle of the volume. That is to say, the normal vector of MSP is the same as one of the coordinate axis. Therefore, we define MSP coordinate C_M as follows,

$$x - axis : \mathbf{x_M} = \mathbf{n}, \tag{2.2}$$

$$y - axis : \mathbf{y_M} = \begin{cases} \mathbf{x_M} \times (\mathbf{y_O} \times \mathbf{x_M}) & \text{if } \mathbf{x_M} \neq \mathbf{y_O} \\ -\mathbf{x_O} & \text{if } \mathbf{x_M} = \mathbf{y_O} \end{cases}, \tag{2.3}$$

$$z - axis : \mathbf{z_M} = \mathbf{x_M} \times \mathbf{y_M}. \tag{2.4}$$
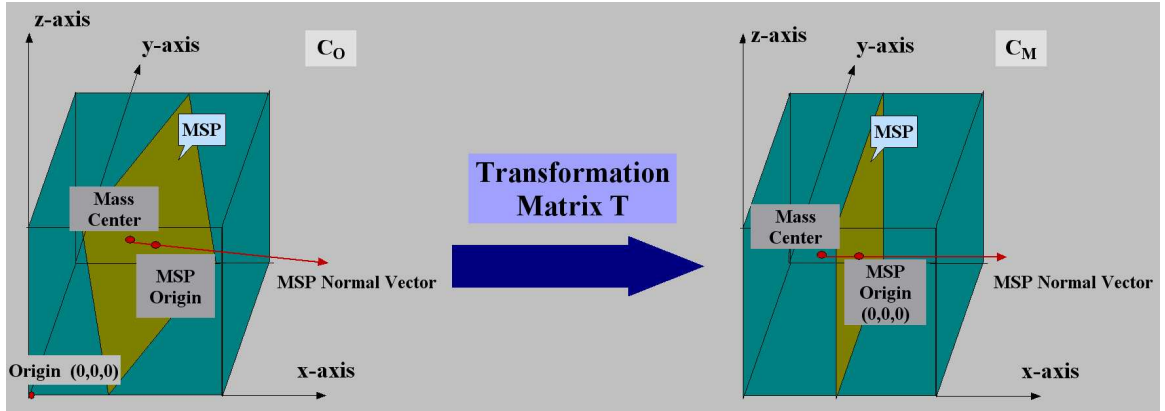
Figure 2.1: **Transformation from input volume coordinate to corrected MSP coordinate.** (Left) When given a input data volume whose MSP is not corrected to be on the mid-line plane. We say that it is in the volume data coordinate C_O. (Right) It is our goal to correct MSP on the mid-line plane. After correcting the brain volume which came from C_O, we say this brain volume is in MSP coordinate C_M.

Otherwise, let MSP origin $\mathbf{o_M}$ be the origin of the MSP coordinate C_M.

Coordinate Transformation : from C_O to C_M

The transformation matrix from C_M to C_O is

$$\mathbf{T_M^O} = \begin{bmatrix} \mathbf{x_M} & \mathbf{y_M} & \mathbf{z_M} & \mathbf{o_M} \\ 0 & 0 & 0 & 1 \end{bmatrix}. \tag{2.5}$$

Thus, the transformation matrix from C_O to C_M is $\mathbf{T_O^M} = (\mathbf{T_M^O})^{-1}$. If we know the apposite $\mathbf{n}$ and $\mathbf{t}$, which determine a MSP and the transformation $\mathbf{T_O^M}$, we can use $\mathbf{T_M^O}$ to correct MSP on the appropriate plane location.

2.3.2   Symmetry Measure

Weighted Cross-corelation

To see how perfect of the object's symmetry, cross-corelation is always the first idea came into our thought. There are two reasons for us to apply weighted cross-corelation instead of general cross-corelation. One of the reason is that the more inner-side the brain, the tissue should be more symmetry. The other reason is based on that most of people have almost perfect symmetry position on both eyes.

Based on these two reasons, different weights on different voxels were given depend on its position. Values of weight were applied by Gaussian curve distribution. Larger weighting values were offered on the inner-side voxels so that these tissues could give a significant influence on symmetry measurement. Oppositely, the more far away from the MSP, the less contribution the voxel made. By experience, range of weight from 1 to 30 was suitable in case.

Voxel-by-voxel multiplication was done while calculating value of cross-corelation. However, it is time consuming if we go through the whole volume data. Besides, there are also several variable regions which vary on each individual subject. Thus, for the reason to reduce computation time and excluding the variable regions, region of interest (ROI) was selected instead of taking the whole volume data into processing. The ROI on x-axis is picked the area inside the skull. Because of the Yakovlevian torque, on y-axis we picked from eyes to the front of the occipital. Along z-axis, we picked from parietal lobe to the top temporal lobe for the sake of the bottom of temporal lobe usually behaves as asymmetry.

According to the above two issues, the weighted cross-corelation value, said WCC, could be written as follows. For each voxel $\mathbf{p_i}$, $\mathbf{q_i}$ is its symmetry point relative to MSP F. Both $\mathbf{p_i}$, $\mathbf{q_i}$ are in ROI and laid on different side of MSP. Vectors $\mathbf{p}$ and $\mathbf{q}$ represent
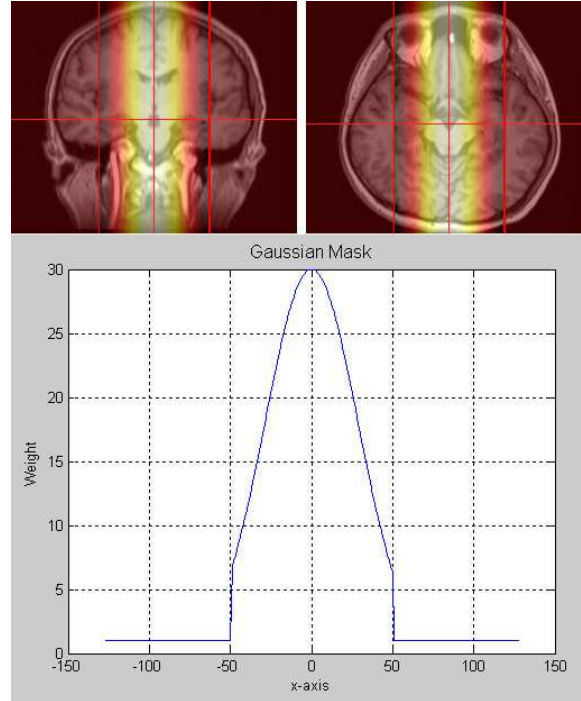
Figure 2.2: **Weighted curve.** (Top brain) The colors which cover the brain means the weighted value. The brighter the color, the larger the value of weight. For the reason that inner-side tissues always present a more precise symmetry. We give these region the major influence which means a larger weighted value. (Bottom curve) Zero on x direction axis indicate the mid-line plane x=0. From x=-50 to x=50 is about the inner-side tissues and also covered both eyes. Thus, we gave a gaussian curve (FWHM=67) weighted value in this place. And the maximum weight is set as 30. Otherwise, we let the region outside x=-50 to x=50 only contribute weight 1.

weighted voxels in ROI on both sides of MSP, respectively.

$$\mathbf{p} = \begin{pmatrix} W(p_1) \cdot I(p_2) \\ W(p_2) \cdot I(p_2) \\ \vdots \\ W(p_n) \cdot I(p_n) \end{pmatrix}, \ \mathbf{q} = \begin{pmatrix} W(q_1) \cdot I(q_2) \\ W(q_2) \cdot I(q_2) \\ \vdots \\ W(q_n) \cdot I(q_n) \end{pmatrix},$$

where $W(\mathbf{v})$ is the weight of voxel $\mathbf{v}$ according to its position, and $I(\mathbf{v})$ is the intensity of voxel $\mathbf{v}$. That is, given a MSP F, value of weighted cross-corelation is considered as

$$WCC(F) = \frac{\mathbf{p} \cdot \mathbf{q}}{\|\mathbf{p}\| \|\mathbf{q}\|}. \tag{2.6}$$

Coronal View   Axial View   Sagittal View
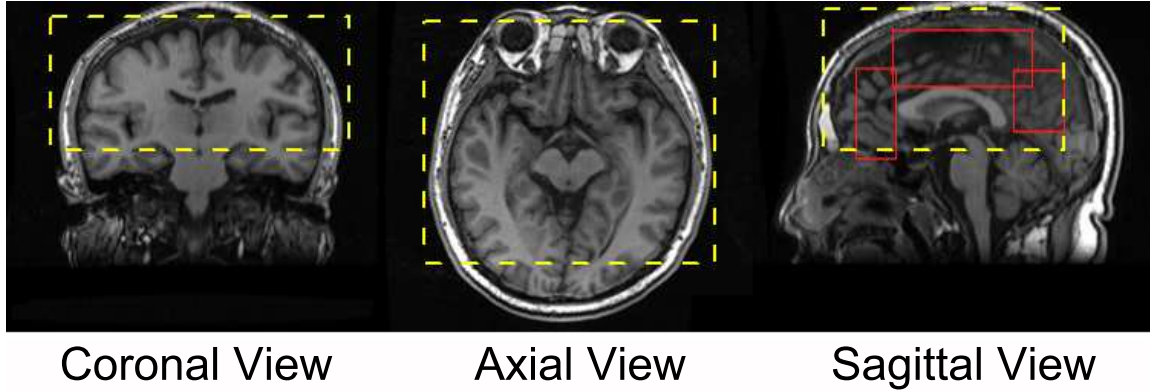
Figure 2.3: **ROI of weighted cross-correlation.** Here shows the area we picked up to calculate cross-correlation value. On x direction, we selected the area inside the skull. On y direction, we selected the area from the eyes to the front of the occipital. Due to "Yakovlevian torque", we exclude occipital lobe. On z direction, we picked from parietal lobe to the top temporal lobe for the sake of the bottom of temporal lobe usually behaves as asymmetry.

For measurement of symmetry, the higher the value of WCC(F) is what we expected.

Darkness of Mid-sagittal Plane

An ideal MSP should contains no brain cortex. That is to say, MSP could bisect right and left hemisphere clear enough. Besides, magnetic resonance images would display black or blurred on the non-tissue region. Thus, if MSP exhibits black or blurred excluding regions of skull, cerebellum, brain stem, corpus callosum and thalamus, it means this MSP may contain little cortex. This is the reason why darkness of MSP was taken as one of our symmetry measurements.

In addition, the region where needs to be focused on MSP is the region excluding skull, cerebellum, brain stem, corpus callosum and thalamus. The region to focused on was selected as region of interest (ROI). We summed up the voxel intensity in ROI, where the summation of intensity on MSP was denoted as DARK. That is, given a MSP F, the
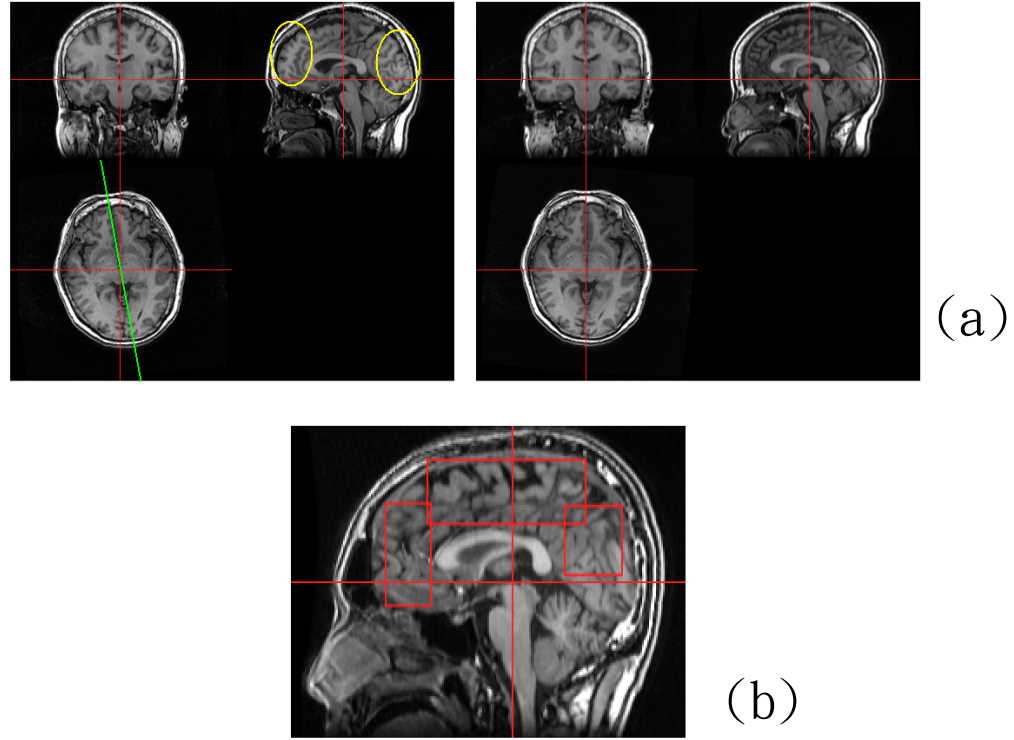
Figure 2.4: **ROI of mid-sagittal plane.** (a) (left) This is a brain volume before MSP correction. The green line indicates MSP on axial view. It is clear that the mid-line plane (the sagittal view) is bright on region of frontal lobe and occipital lobe (the yellow circles) for mid-line plane crossing through brain cortex. (right) This is a brain volume after MSP correction. MSP of brain is set as the mid-line plane (the sagittal view). We can observe that MSP is more blurred than the left one except the bright occipital lobe caused by Yakovlevian torque. (b) An ideal MSP should contains no brain cortex on it. Additionally, MR images would be black or blurred if there is no tissue on it. Thus, we selected three regions (three red squares) that cortex may show on as ROI and summing up voxel intensity in it. The lower the summation of intensity means there is little cortex exists on this MSP.

equation is represented as

$$DARK(F) = \sum_p I(\mathbf{v}), \qquad (2.7)$$

for $\mathbf{v} = (x, y, z) \in ROIonF$ and $I(\mathbf{v})$ is intensity of voxel $\mathbf{v}$. For measurement of a good MSP, the lower the value of DARK(F) is what we expected.

2.3.3 Parameter Estimation

Initial Condition

Referring to equation 2.1, we have known that MSP F is determined by two variables, distance from $\mathbf{m_C}$ to $\mathbf{o_M}$, t, and normal vector, $\mathbf{n}$. For variable t, we simply consider that an ideal MSP is always cross mass center $\mathbf{m_C}$. Therefore, the initial value of t was set to be zero. Two different conjectures were then used to determine the initial normal vector n of each subject. The values of objective function

$$Obj_{t,\mathbf{n}} = WCC(F) + \alpha \times DARK(F). \tag{2.8}$$

based on the these two conjectures were calculated. The one which had smaller value objective function was selected as the initial normal vector of this subject.

The first conjecture of normal vector is set as x-axis in coordinate C_O, which is

$$\mathbf{n_1} = \mathbf{x_O}. \tag{2.9}$$

Second, we referred Tuzikov, Colliot, and Bloch [39, 40]'s method. Imaging the human brain as an ellipsoid, by Goldstein's theory[10], the principle inertia axes of the ellipsoid is defined by the eigenvectors of the corresponding covariance matrix. The corresponding covariance matrix C is about the mass center $\mathbf{m_C}$.

$$m_{pqr}(f) = \int \int \int_{F} f(x,y,z)(x - x_c)^p (y - y_c)^q \times (z - z_c)^r dx dy dz. \tag{2.10}$$

$$C \;=\; \begin{pmatrix} m_{200} & m_{110} & m_{101} \\ m_{110} & m_{020} & m_{011} \\ m_{101} & m_{011} & m_{002} \end{pmatrix}. \tag{2.11}$$

There are three eigenvectors of covariance matrix C. These three eigenvectors, $\mathbf{u_1}, \mathbf{u_2}, \mathbf{u_3}$, indicate three principle axes of ellipsoid. The one which was closest to axis $\mathbf{x_O}$ was the second conjecture of plane normal vector $\mathbf{n}$, which is

$$\mathbf{n_2} = \arg\min_{\mathbf{u}\in\{\mathbf{u_1},\mathbf{u_2},\mathbf{u_3}\}} \{ang(\mathbf{u}, \mathbf{x_O})\}, \tag{2.12}$$
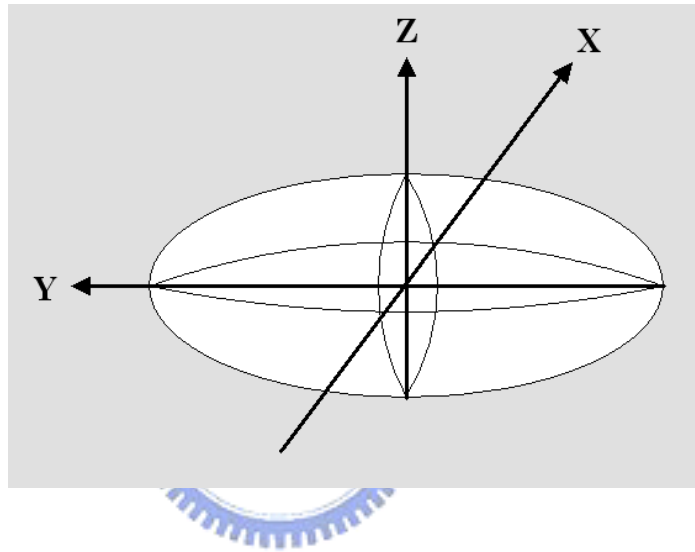
Figure 2.5: **Principal inertia axes.** Imaging the human brain as an ellipsoid, we could use Goldstein's theory to find out the axes of the ellipsoid of inertia [10]. Then, we chose one of the axis which closed to $\mathbf{x_O}$ as the initial value of plane normal vector $\mathbf{n}$.

Two measurements of normal vector were calculated for each subjects, the one which lead to smaller value of objection value with $t = 0$ was selected as the initial normal vector $\mathbf{n}$ of the subject.

$$\mathbf{n} = \arg\min_{\mathbf{n}\in\{\mathbf{n_1},\mathbf{n_2}\}} \{Obj_{0,\mathbf{n}}\}. \tag{2.13}$$

Optimization Method

After deciding the initial values of parameters, optimization process was applied for parameter estimation. Since we have already got a feasible initial value of the normal vector about the MSP, there is no doubt that even a optimization method which may fall into local

minimum could fulfill our requirement. It seems that the downhill simplex optimization method usually works well. For this reason, we chose the downhill simplex optimization as optimization method for parameter estimation.

As described above, two criteria, weighted cross-corelation (WCC) and darkness of MSP (DARK), were considered to measure MSP. The higher the weighted cross-correlation value (WCC) and the lower the summation of intensity (DARK) is what we expected. Thus, given a mid-sagittal plane *F*, the optimization routine is tempted to minimize the objective function,

$$Obj_{t,\mathbf{n}} = WCC(F) + \alpha \times DARK(F).$$

According to our experience, good results could be obtained while the α value was set as -0.00219.

Chapter 3

Template Construction

3.1   Introduction

A brain template is a reference volume that stands as a standard coordinate. To construct a brain template, we may think intuitively to average all the volume data in our database. However, due to diversities of scanning poses and brain sizes, a registration procedure is needed before the overall averaging. Therefore, the brief construction steps is as follows.

1. Brain Registration

2. Averaging

3. Smoothing

3.2   Brain Registration

For medical brain image data, registration is to align different brain volumes together. Sometimes, it is also called "spatial normalization". In addition, we could consider that registration is an essential process of comparing different brain volumes. In neuroscience researches, there are various applications of registration, such as analysis of functional images, detection of the difference between normal and abnormal volume data, changes of disease state over time, so on and so forth. For medical image registration method, many criteria (list in table 3.1) govern the final form of registration process[26, 44, 5]. The case in our work results in inter-subject, MR to MR, 3D to 3D. Other criteria left to be the choices of our consideration.

Within the steps of template construction, it is necessary to preserve the uniqueness of each brain subject. Therefore, we develop a linear transformation method for registering all the brain volumes together instead of a nonlinear process which usually distort volume by bending the brain tissue.

Registration Criteria	Example
Subject	inter-subject[13], intra-subject
Modality of source and target	CT to CT, MR to MR[21], PET to PET,
	CT to MR, CT to PET, etc.
Dimensionality	2D to 2D, 2D to 3D, 3D to 3D
Transformation model	rigid, affine, piecewise affine, non-linear[4]
Basis of registration	landmark-based, segmentation-based[16, 33],
	surfaced-based[35], voxel-based, etc.
Similarity measurement	mutual information[42] , cross-correlation[19] , etc.
Optimization method	Newton method, Simplex method, etc.

Table 3.1: **Registration Criteria.**

In this section, we bring up our idea of brain registration. At first, we need to select several mapping features, such as mapping point, mapping line and mapping plane. Undoubtedly, the mapping plane would be MSP. By referring to the Talairach coordinate, we select anterior commissure (AC) as the mapping point, as well as the line passing through AC and posterior commissure (PC), said AC-PC line, as the mapping line. After aligning all these features together, we scale the brain volumes to a determined size.

To build up a general standard, we first select a representative brain as the reference volume. That is, all subjects will refer the features on representative brain. The second step is to transform representative brain's AC and PC onto individual brain by applying the transformation matrix which follows Umeyama theory [41]. Every individual brain will map transformed AC and transformed AC-PC line together. Then all brain subjects will scale to the same size as representative brain. The brief processing steps of brain registration is like this :
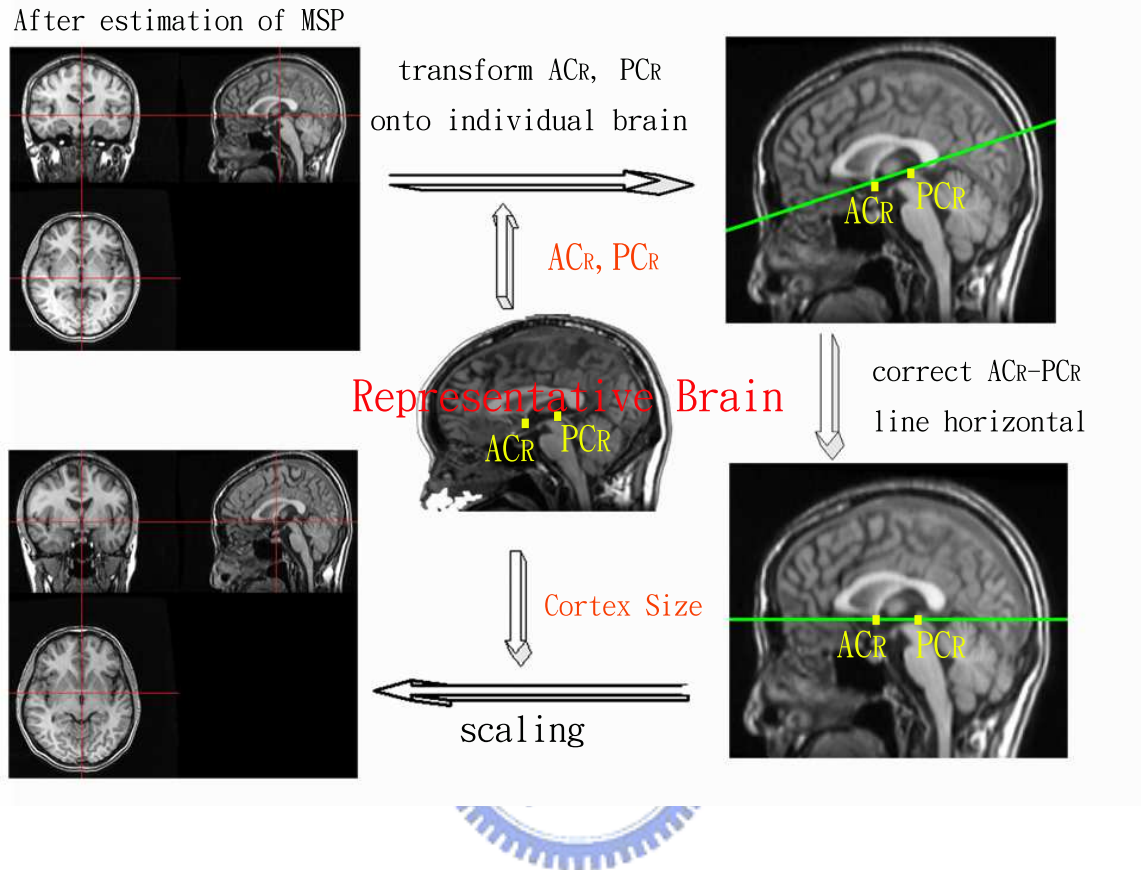
Figure 3.1: **Registration.** On the basis of representative brain, we transform representative brain's AC and PC onto every individual brain, and denote the transformed AC, PC as AC_R, PC_R (the yellow points). Consequently, we translate AC_R on a determined position and correct $AC_R - PC_R$ line (the green line) horizontal in order to map all the subjects together. After scaling each individual brain to the same size as the representative brain, we create a brain template by averaging all brain subjects.

1. Determination of representative brain

2. Transformation of AC_R and PC_R from representative brain to every individual brain

3. Mapping of AC_R and $AC_R - PC_R$ line on every individual brain

4. Scaling of every individual brain according to the representative brain

3.2.1   Determination of Representative Brain

In Talairach coordinate, AC and PC are critical landmarks of coordinate definition. In other words, these two landmarks also play important role of volume registration. As described before, we select AC as the mapping point and AC-PC line as the mapping line. However, these two structures are too close that only 25 mm between them. Once a slight displacement occurred, a significant angular error of AC-PC line would be arose. It is not our expectation to rise up such an unstable situation.

In order to diminish the instability of displacement and subjectivity of landmark selection, a representative brain would be chose as a reference volume, as well as its features and sizes will be the reference of other brains. It is our plan to transform representative brain's AC and PC onto all the other volumes, and denoted as AC_R, PC_R. The goal is to take AC_R as the mapping point and $AC_R - PC_R$ line as the mapping line.

As mentioned above, the role that a representative brain plays is served as a reference volume, such as its brain size and features. There are several choices to select a representative brain. One is the Talairach brain, and the other is the mean brain volume which is constructed by averaging every subject warped to the Talairach brain. However, both the warping variation is too large for each brain subject. It might be caused by different races. Thus, we abandon to use Talairach brain as a standard reference brain volume and plan to choose a volume which has the minimum sum of magnitude with each subject.

A representative brain should hold healthy tissues which do not appear any decayed parts. For this reason, we decided to select the representative brain in the prime of life, which ranges from age 18 to 35.

Given a group of age between 18 to 35, each brain among this group was chose as template once. As one subject was selected as the template, all the other brains in this group were normalized to this template. Magnitude of deformation field from normalized

brain to original brain were calculated for all the other subjects. Then, we summed up these magnitude values. For each brain as template, it has a summed magnitude value of other subjects. The brain which hold the smallest value of summed magnitude was selected as the representative brain.

For every subject i,

$$D_i = \sum_j def(s_i, s_j), \qquad i \neq j, \tag{3.1}$$

where $def(s_i, s_j)$ is the deformation field between subject i and subject j. The subject which has minimum sum of magnitude D_i with all the other subjects is chose as the representative brain.

3.2.2   Determination of the Mapping Point and Mapping Line

Since Evans et al. [6] have found out that by determining several landmarks, AC-PC line could be well estimated. Based on Evans et al.'s conclusion, genu (GU), inferior margin of thalamus (TH), splenium (SP), superior cerebellar margin (CB) and occipital pole (OP) are good enough to estimate AC-PC line. Figure 3.2 shows positions of these five landmarks.

In order to diminish the distortion caused by transformation and to preserve location of AC-PC line, these five landmarks are took as the critical pattern when calculating the transformation matrix. Additionally, Arun, Huang, and Blostein [3] have given an solution on least-squares fitting of two 3D point sets. Unfortunately, it failed in some cases. Subsequently, Umeyama [41] proposed a more strictly theorem on this problem. As the result of our tests, Umeyama's theorem indeed give reasonable transformation matrix between two 3D point sets. Therefore, given two sets of five landmarks, a transformation matrix which could map these two sets of landmarks approximately together is obtained by Umeyama's theorem. Consequently, we transform representative brain's AC and PC onto individual brain by this transformation matrix and denote the transformed AC, PC as AC_R, PC_R. In
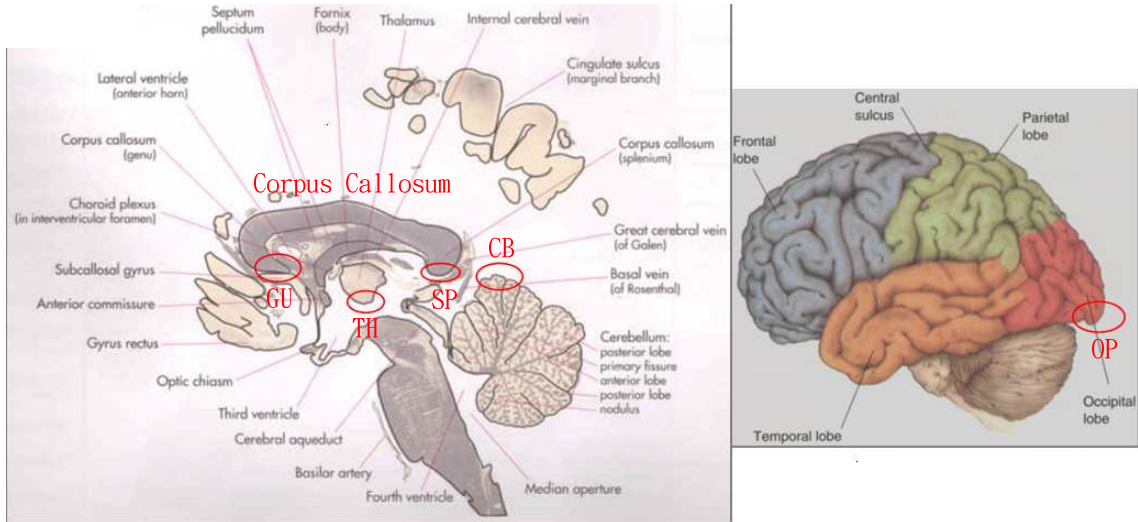
Figure 3.2: **Landmarks.** The five landmarks which can approximately fit a line close to AC-PC line are genu (GU), inferior margin of thalamus (TH), splenium (SP), superior cerebellar margin (CB) and occipital pole (OP) [6].

the end of this step, AC_R is the mapping point and the line passing through AC_R and PC_R is the mapping line, called the $AC_R - PC_R$ line.

In this paragraph, we state the procedure of landmarks selection. For the reason that landmarks are brain tissues, they are always occupied not only one voxel in volume data. Therefore, we define labelled positions of every landmarks for the experts to obey while marking landmarks on all volume subjects. Nevertheless, it could be happened that expert may labelled different positions according to the pitch angle of brain as figure 3.4 shows. In order to label the similar location of each landmarks relatively on every subjects, we decided to correct AC-PC line horizontally first. That is to say, the working routine of landmark selection is as follows :

1. Labels of AC and PC

2. Set AC-PC line horizontal

3. Labels of GU, TH, SP, CB and OP

Representative subject **Individual subject**
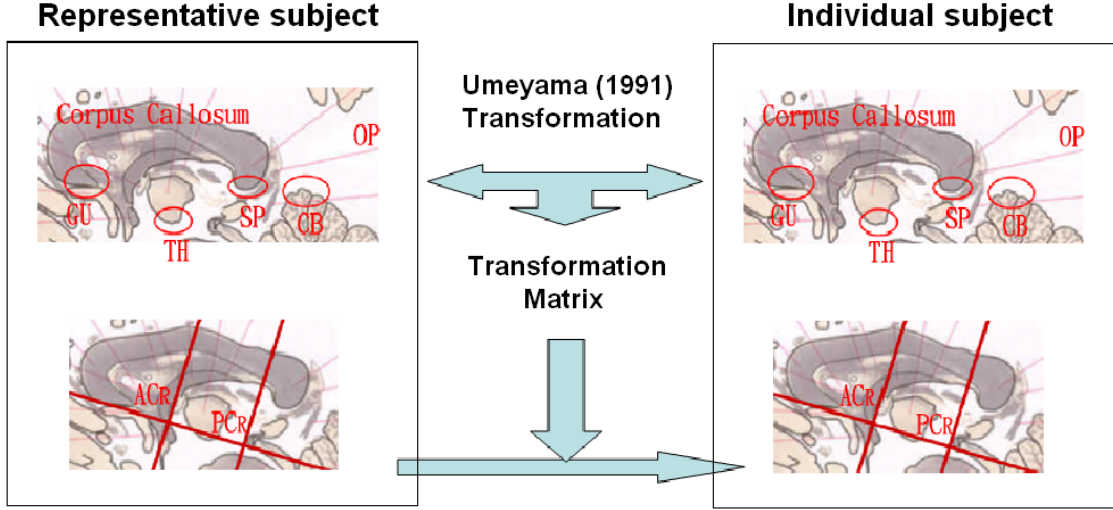
Figure 3.3: **Transformation from representative brain to individual brain.** Once we obtained the transformation matrix by Umeyama transform of two sets of landmarks, we transform the AC, PC points from representative brain to the individual brain and denoted as AC_R, PC_R.

Moreover, we list the defined labelled position of landmarks in table 3.2.

Further on, we should notice that the definition of occipital pole in medical is the most posterior promontory on both cerebral hemisphere. However, a landmark on MSP is what on demand. Thus, a landmark on MSP which could in behalf of occipital pole should be defined. Intuitively, the intersection point of MSP and the line cross both occipital pole is set as the landmark which represent as occipital pole. Assume the corrected MSP is $x = d$ in volume coordinate. The labelled position of occipital pole are $P_A(x_A, y_A, z_A)$ and $P_B(x_B, y_B, z_B)$. The line passing through P_A and P_B is

$$
\begin{bmatrix} x \\ y \\ z \end{bmatrix} = \begin{bmatrix} x_A \\ y_A \\ z_A \end{bmatrix} + t \begin{bmatrix} x_B - x_A \\ y_B - y_A \\ z_B - z_A \end{bmatrix}, \qquad for \quad -\infty \le t \le \infty. \tag{3.2}
$$

Tissue Name	Labelled Position
Anterior commissure (AC)	Superior and posterior margin
Posterior commissure (PC)	Inferior margin
Genu (GU)	Inferior margin
Thalamus (TH)	Inferior margin
Splenium (SP)	Inferior margin
Cerebellar (CB)	Superior margin
Occipital pole (OP)	Extreme promontory on both hemisphere

Table 3.2: **The landmark labelled position.**

Therefore, the intersection point $P_C(x_C, y_C, z_C)$ is

$$
\begin{bmatrix} x_C \\ y_C \\ z_C \end{bmatrix} = \begin{bmatrix} x_A \\ y_A \\ z_A \end{bmatrix} + t \begin{bmatrix} x_B - x_A \\ y_B - y_A \\ z_B - z_A \end{bmatrix}, \qquad for \quad t = \frac{d - x_A}{x_B - x_A}. \tag{3.3}
$$

P_C is the landmark which stands for occipital pole on MSP.

3.2.3 Scaling

Due to different volume images and different sizes of the individual brains, there still left one thing to be processed before the overall averaging. For every subject, we have done the rotation and translation. Therefore, the remaining thing of transformation left only the scaling. Thus, after mapping all AC_R points together and correct $AC_R - PC_R$ line horizontal, we piecewise scale each individual subject to the same size as the representative brain subject's.

Our model is defined similar to the Talairach coordinate. AC_R is set as origin. $AC_R -$

PC_R line, VAC_R line and the line perpendicular to the above two lines are set as three axes. Based on the origin, AC_R, five directions stretch out along three axes are served as measurements of scaling. We labeled edges of cortex on these extend directions. Figure 3.5 illustrates these five labeled positions. For each subjects, we extend the voxel size to the same size as representative brain's according to its direction. For example, assume the length of line segment from AC_R extend to cortex border along $AC_R - PC_R$ line is l_r cm on representative brain and the length of same line segment on individual brain is l_s cm. The scaling measurement of this direction on individual brain is $\frac{l_r}{l_s}$. As the result, every subject would be the same size as the representative brain.

3.3 Averaging and Smoothing

After scaling, all brain subjects would have same sizes. Therefore, at the last step, all subjects were averaged and the resulting averaged volume was considered as the brain template.

Besides, for the benefit of increasing signal-to-noise (SNR) ratio, smoothing is also performed. Moreover, by central limit theorem, smoothing could modulate errors of normalization in a normal distribution to ensure the subsequent inference test more accurate. Here, we applied an isotropic Gaussian kernel with FWHM = 8mm.
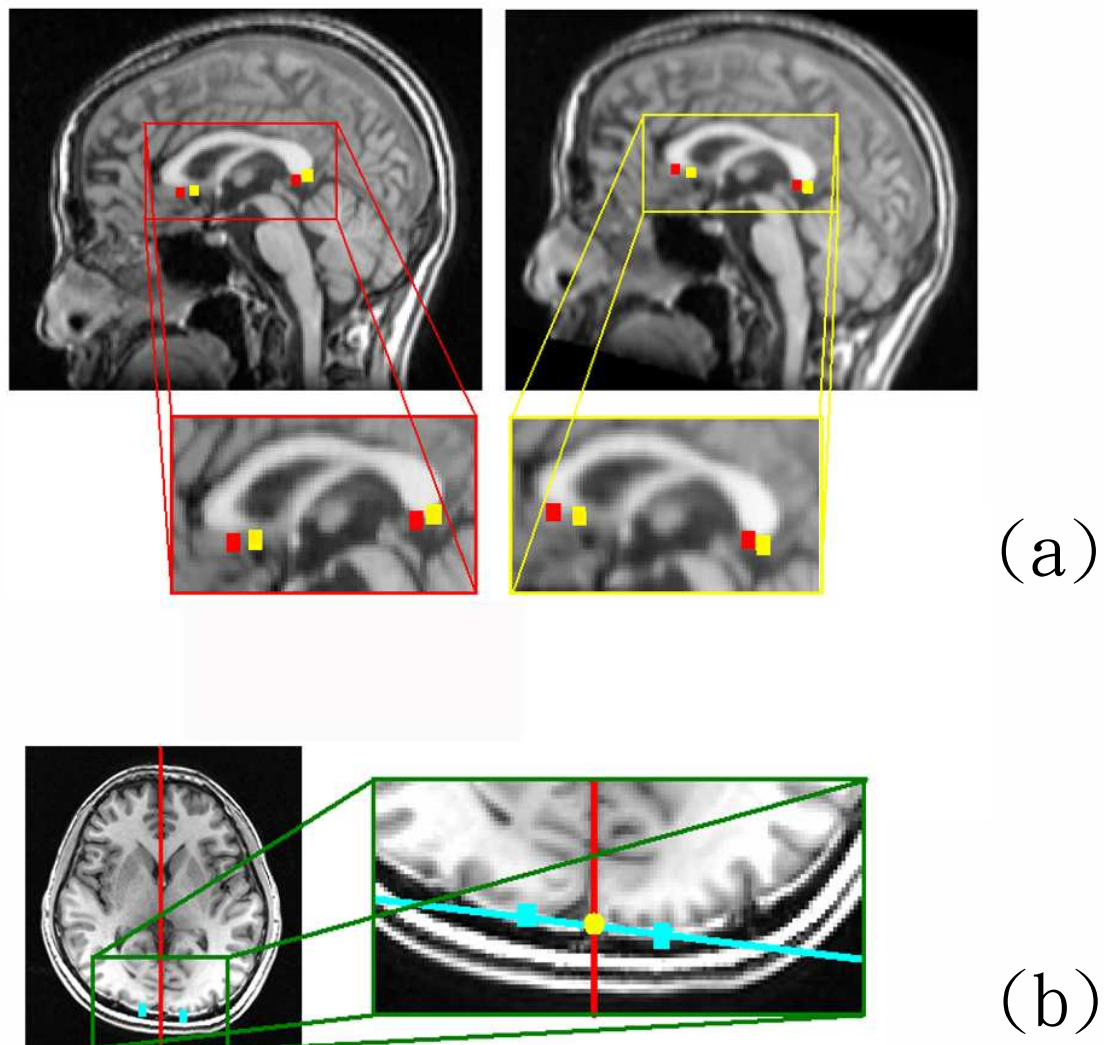
Figure 3.4: **Determination of genu, splenium and occipital pole.** (a) In this figure, we use genu and splenium to explain the pitch angle could effect the labelled position of landmarks. The defined labelled position of genu and splenium is inferior margin. Taking a view of the left brain, the original volume, the red voxels are the labelled position of these two landmarks. On the other hand, we rise up the brain for some degree, and the labelled position are as yellow voxels shows. Here we affirm the instability of landmarking if we don't assign some specified positions of landmark pattern. (b) The landmark position of occipital pole on MSP is illustrated in this figure. The most posterior promontory on both cerebral hemisphere is the definition of occipital pole in medical. Here we marked the occipital pole (the blue ones). In order to attain a landmark on MSP as well as this landmark could in behalf of occipital pole. The crosspoint of MSP and the line which goes across the occipital pole is set as the landmark of occipital pole (the yellow one).
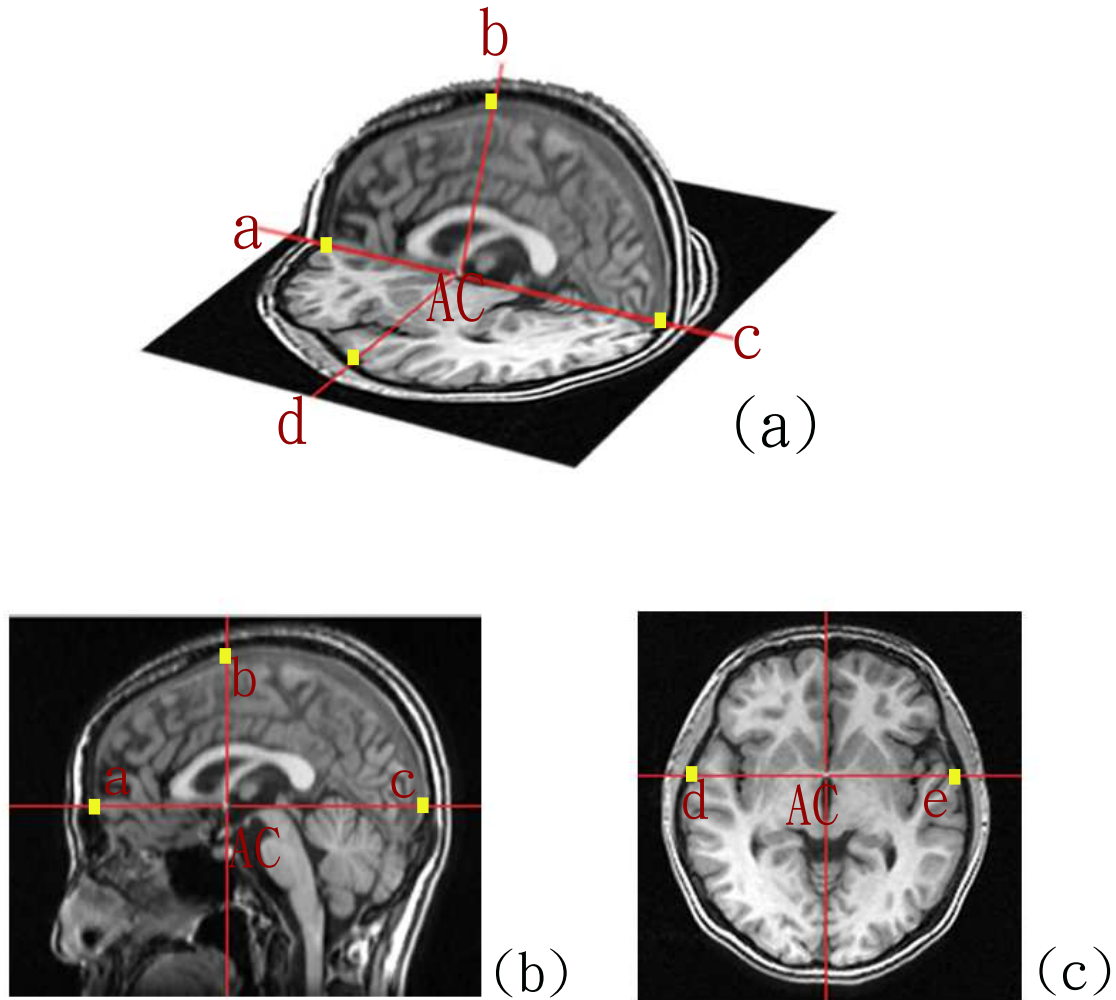
Figure 3.5: **Bounding box.** (a) For that AC is a critical feature in brain volume coordinate, five directions extended from AC have been chosen to be the ruler of scaling. In figure (a)(b)(c), we point out these five line segments, which are AC to a, AC to b, AC to c, AC to d and AC to e. (b) We spotted points a, b and c on sagittal view just as figure (b) shows. Along AC-PC line, the intersection points (the yellow spots) of AC-PC line and the borderline on cortex are denoted as a and c. On the other hand, along the vertical line which perpendicular to AC-PC line, the border point (the yellow spot) of cortex is denoted as b. (c) This figure shows two more intersection points (the yellow spots) on axial view. These two crossing points, denoted as d and e, are the cortex border points along the horizontal line which also perpendicular to the AC-PC line.

Chapter 4

Results

4.1 Materials

All volume data are collected by Taipei Veterans General Hospital. The magnetic resonance images are obtained from the same GE 1.5-Telsa MRI scanner, Excite/Excite HD platform, which set up with TR=8.672 ms, TE=1.86 ms, FOV = $26 \times 26 \times 10$ cm^3, matrix size=$256 \times 256 \times 124$, voxel size=$1.02 \times 1.02 \times 1.5 mm^3$ and phase FOV=0.7. The effects of head motion were minimized by using a head-neck pad and the fine modulation manually done by the professional.

There are totally 58 subjects (age : 24.1207 ± 4.5848) in our brain MRI database, including 28 males (age : 25.4286 ± 4.2376) and 30 females (age : 22.9 ± 4.6264). The range of age is between 18 to 35. Table 4.1 shows the distribution of each age group. Additionally, there was no subjects with tumor and infarction. Any abnormal brain subjects were excluded from this study. All of the volume data provided by Taipei Veterans General Hospital were originally saved in Dicom format. Before dealing with our procedures, MRIs were transferred into Analyze format. The mean intensity of these 58 subjects is 192.7042 ± 22.8773 originally. In addition, range of intensity is 0-3863.

	Age		
	18-20	21-30	31-35
Male	3	21	4
Female	12	15	3

Table 4.1: **Number of subjects in each age group.**
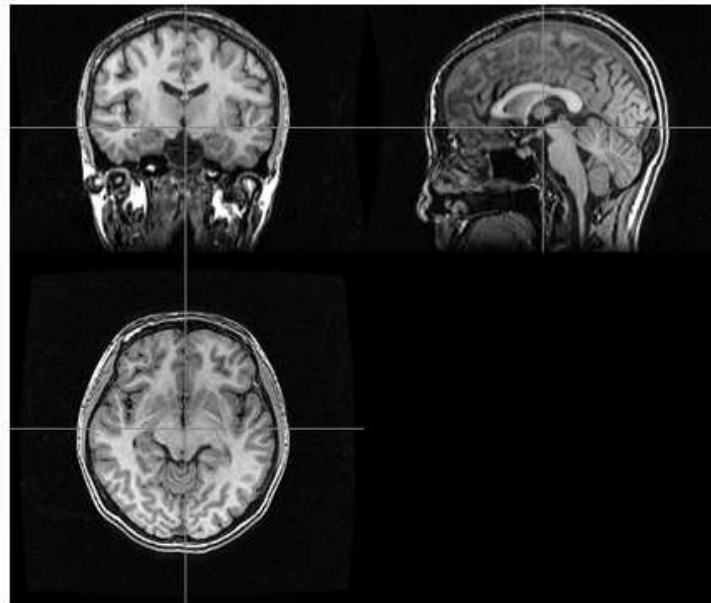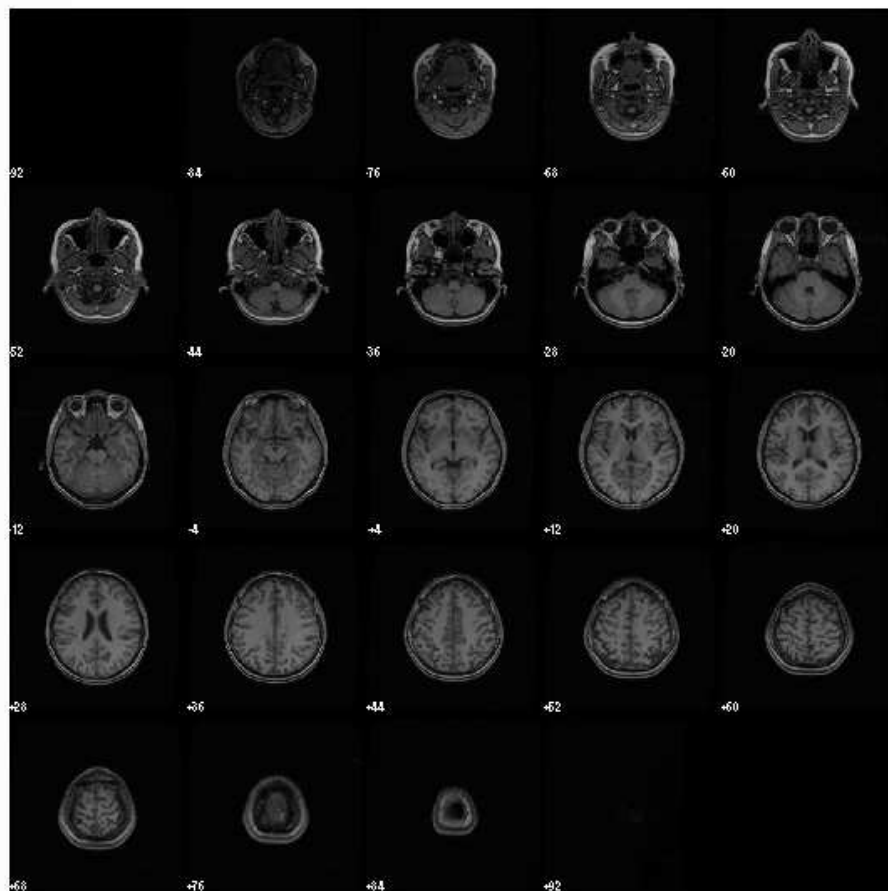
Figure 4.1: **MR volume.** The image volume has dimension 256×256×124, voxel size 1.02×1.02×1.5mm^3 and was saved in 16-bit integer , little-endian. (a) Views from three directions. (b) The axial views.

4.2 Estimation of Mid-sagittal Plane

The MSP auto-estimation algorithm was primarily implemented in Matlab 7.0, accompanied with C++ in order to accelerate speed. This process was ran on Windows XP platform with AMD Athlon (TM) XP 2800+ (2.08 GHz CPU and 1GB RAM), whereas the average computation time was 202.8173 seconds for 58 normal subjects.

4.2.1 Validation by Experts

It is difficult to verify if a MSP is perfect, for MSP has no exactly definition. Therefore, we ask the expert to identify if the MSP is good enough on medical diagnosis. Table 4.2 lists the fine-tuning done by the expert. The mean absolute value of fine-tuning angle of yaw and roll angle are 0.0126 degree and 0.0216 degree. In addition, the mean value of fine-tuning translation is 0.6897 mm.

	Fine-tuning Results		
Result	Yaw angle (deg.)	Roll angle (deg.)	Translation (mm)
Mean	0.0126	0.0216	0.6897
Var.	0.00020898	0.00025194	0.4985
Std.	0.0145	0.0159	0.7060

Table 4.2: **Fine-tuning of the auto-estimated MSP by the expert.**

Because MSP has no exact definition in clinical, there are always several choices for MSP determination. Here we show up neighbor x-direction planes in order to explain why mean value of translation for MSP auto-estimation is 0.6897 mm. Figures (a),(b),(c) are

x=127,x=128, x=129, respectively and the auto-estimated MSP is plane (b). We could observe that in plane (a) and (c), the cortex region is also blurred and dim as plane (b). It is caused by the wide space between left and right hemisphere. Thus, if we only consider the darkness of MSP, determination of MSP is various. In our MSP auto-estimated method, there are two criteria, WCC and DARK, to be considered. Program would select a plane which is the one best fitting the criteria objectively. Since we have considered the darkness of MSP, if there is a wide space between left and right hemisphere, determination of MSP would be affected. At this moment, the critical factor to determine a MSP is depend on other features, for example, AC, the tunnel between the third ventricle and the forth ventricle, etc. It is depend on personal subjectivity. Thus, fine-tuning on translation seems not so stable for mean value is 0.6897 mm and the standard deviation is 0.7060.

Here we propose a case to explain the judgment of MSP estimation from the expert and MSP auto-estimation method. Figure 4.3 shows three volume images, top (a) is the original data obtained from hospital, middle (b) is the volume which processed after MSP auto-estimation method, bottom (c) is the volume corrected from (b) by the expert. To make a comprehensive survey on (b) and (c), it seems that MSP corrected by the expert (sagittal view of figure 4.3(c)) is brighter than the auto-estimated MSP (sagittal view of figure 4.3(b)). However, if we examine in a more detailed view, the brighter region of the expert-corrected MSP is occipital lobe, which means this brighter region is caused by Yakovlevian torque. In addition, the tunnel connected the third ventricle and the forth ventricle is also a criterion to identify a MSP. In figure 4.3(b) and (c), we could realized that this tunnel clearly reveals in expert-corrected MSP but not in auto-estimated MSP. For that Yakovlevian torque is a normal phenomenon in human brain and the tunnel also appear in (c), the expert therefore select sagittal view in (c) as MSP.

(a) x = 127

(b) x = 128

(c) x = 129
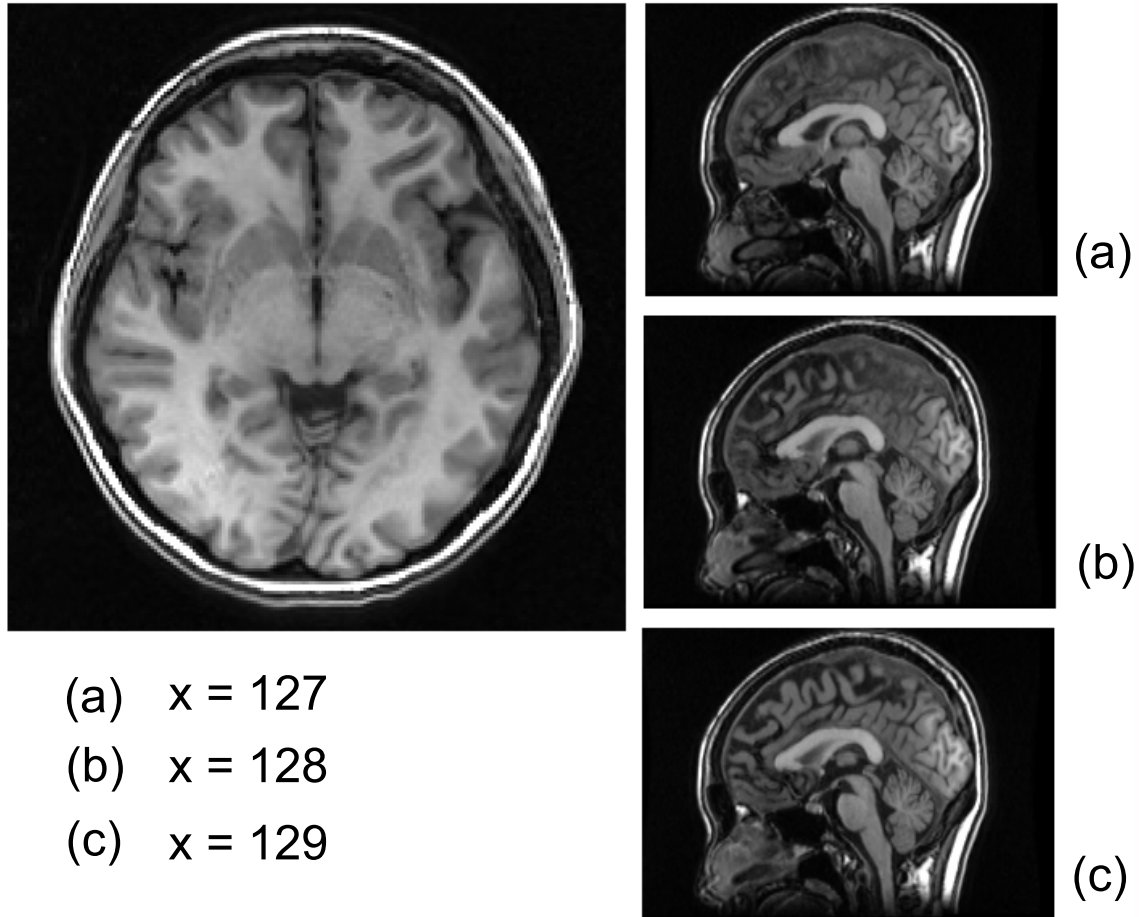
Figure 4.2: **Translation measured by MSP auto-estimation.** Because MSP has no exact definition in clinical, there are always several choices for MSP determination. Here we show up neighbor x-direction planes in order to explain why mean value of translation for MSP auto-estimation is 0.6897 mm. Figures (a),(b),(c) are x=127,x=128, x=129, respectively and the auto-estimated MSP is plane (b). We could observe that in plane (a) and (c), the cortex region is also blurred and dim as plane (b). It is caused by the wide space between left and right hemisphere. At this moment, the critical factor to determine a MSP is depend on other features, for example, AC, the tunnel between the third ventricle and the forth ventricle, etc. It is depend on personal subjectivity. Thus, fine-tuning on translation seems not so stable for mean value is 0.6897 mm and the standard deviation is 0.7060.
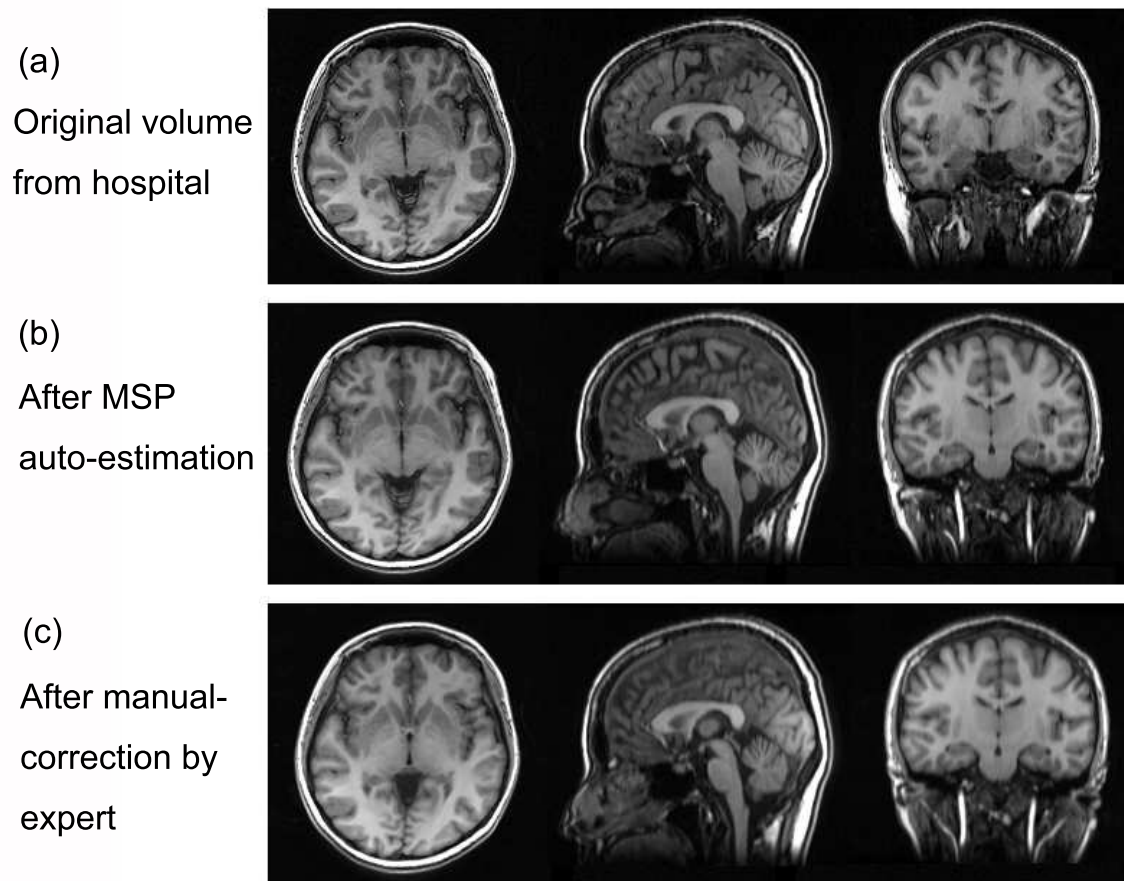
Figure 4.3: **Auto-estimation MSP and expert-corrected MSP.** (a) Original volume data obtained from hospital. (b) Volume data after auto-estimation method. (c) Volume data after correction from (b) by the expert. Although auto-estimated MSP (sagittal view in (b)) seems darker than expert-corrected MSP (sagittal view in (c)), the expert-corrected MSP clearly reveals tunnel between the third ventricle and the forth ventricle. Because the bright region is caused by Yakovlevian torque and the tunnel is also a criterion to identify MSP, the expert therefore determined MSP in (c) is better than MSP in (b).

4.3 Construction of Brain Template

The whole template construction procedure was implemented primarily in Matlab 7.0 and secondarily in C++ on account of computation time. The computation platforms were Windows XP and Linux system.

We constructed three templates (Female, Male and both gender) by following our method described before, and then smoothing with 8mm isotropic Gaussian kernel. Otherwise, templates of gray matter (GM), white matter (WM) and cerebral spinal fluid (CSF) were also created. All these templates are showed in figure 4.7.

4.3.1 Brain Templates

58 normal adult subjects were taken to construct Taiwanese brain template by our proposed method. Age range is from 18 to 35 years old (24.1207 ± 4.5848). And the selected representative brain is a 23-year-old male brain. After averaging, we smoothed the resulting averaged volume by a 8mm isotropic Gaussian kernel in order to obtain a smoothed brain template.

Gender Templates

We also constructed brain templates for both gender groups. There are 28 males (age : 25.4286 ± 4.2376) and 30 females (age : 22.9 ± 4.6264) in our database. The representative brain for male group is a 26-year-old female brain. Additionally, the representative brain for male group is the same brain as for both gender group, a 23-year-old male brain. A 8mm isotropic Gaussian kernel applied on these two gender templates as well.

Figure 4.4: **Taiwanese Template.** 58 normal adult subjects were taken to construct Taiwanese brain template by our proposed method. Age range is from 18 to 35 years old (24.1207 ± 4.5848).

Figure 4.5: **Taiwanese Male Template.** 28 normal male adult subjects were taken to construct Taiwanese brain template by our proposed method. Age range is from 18 to 35 years old (25.4286 ± 4.2376).
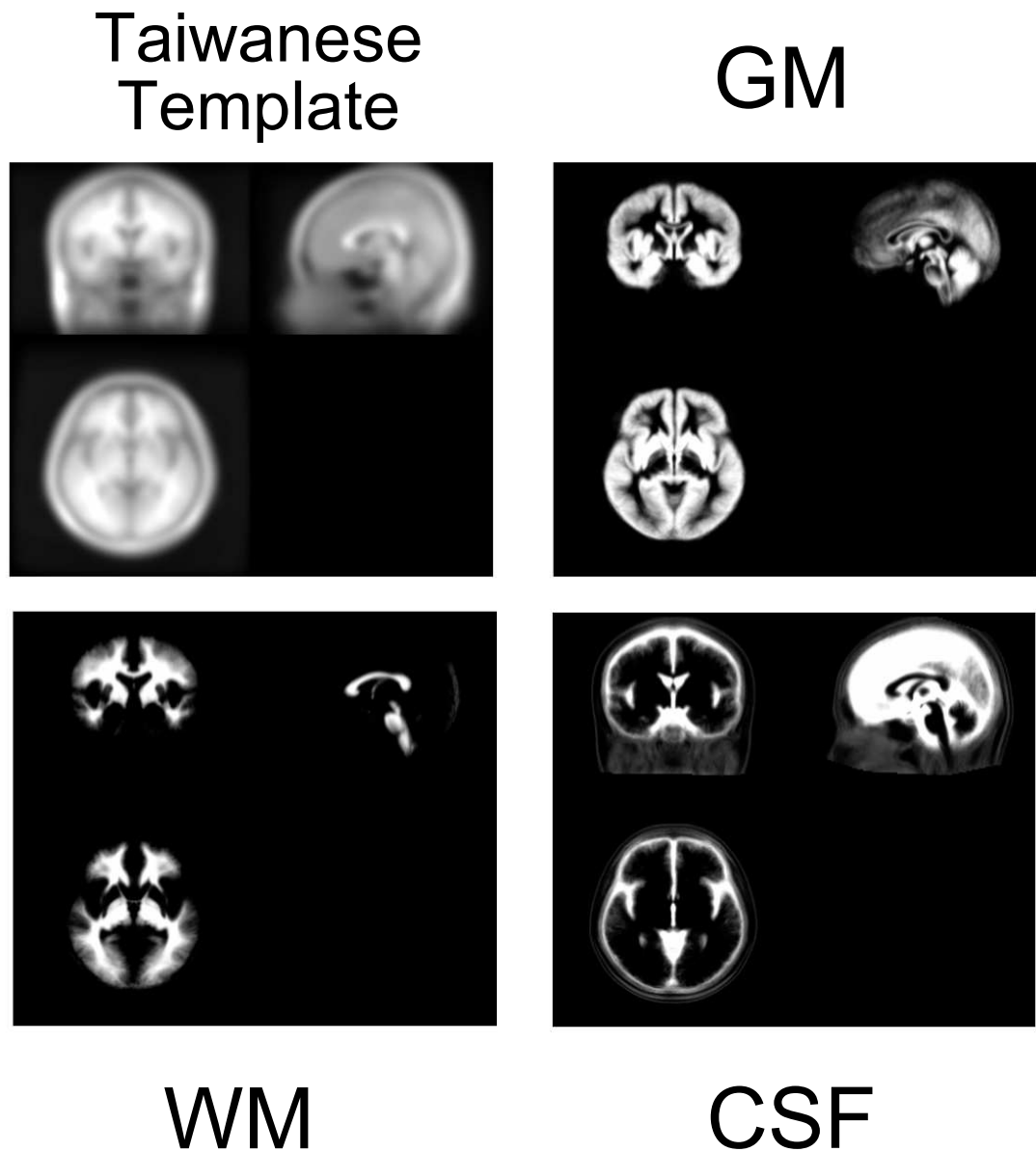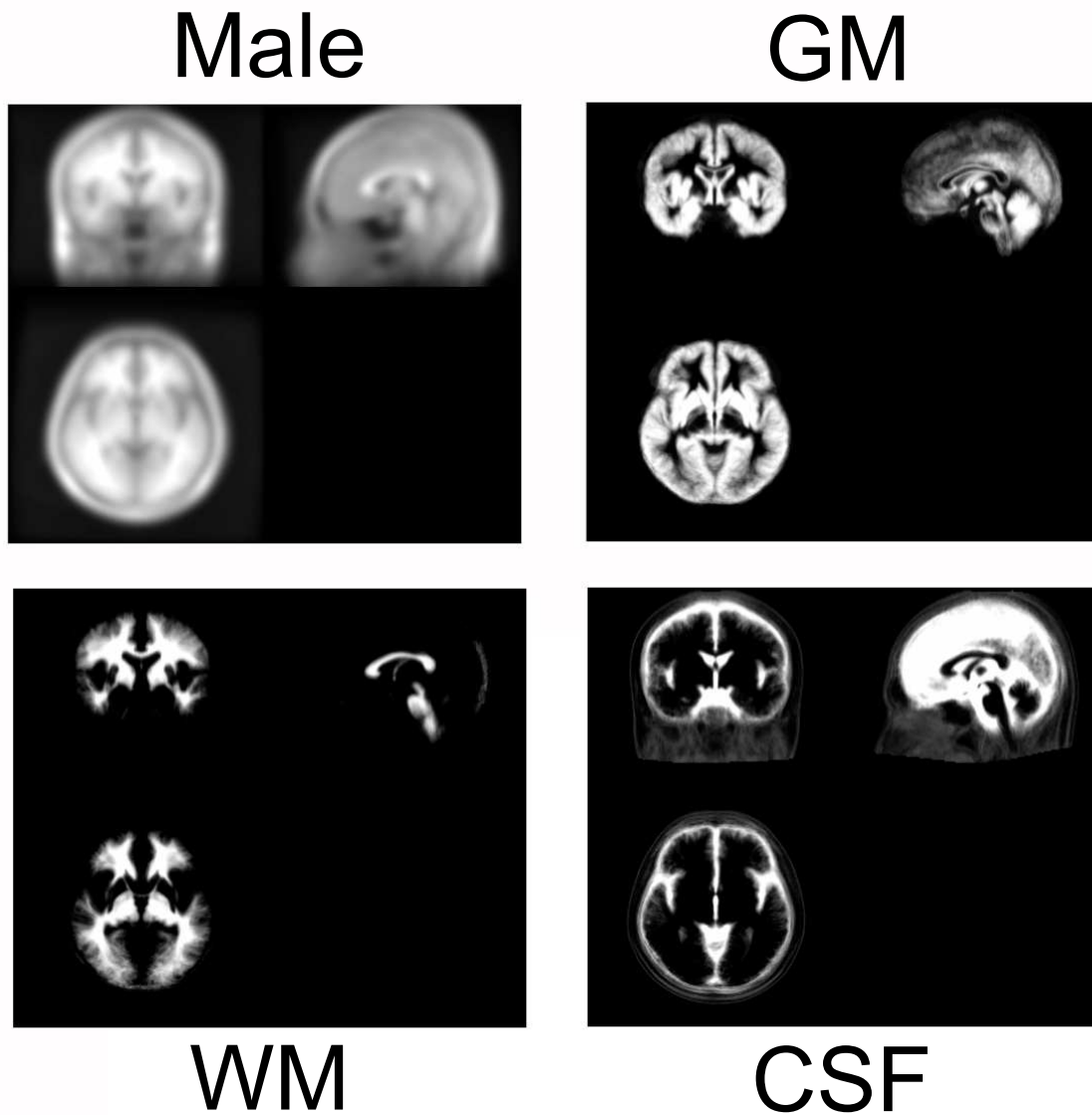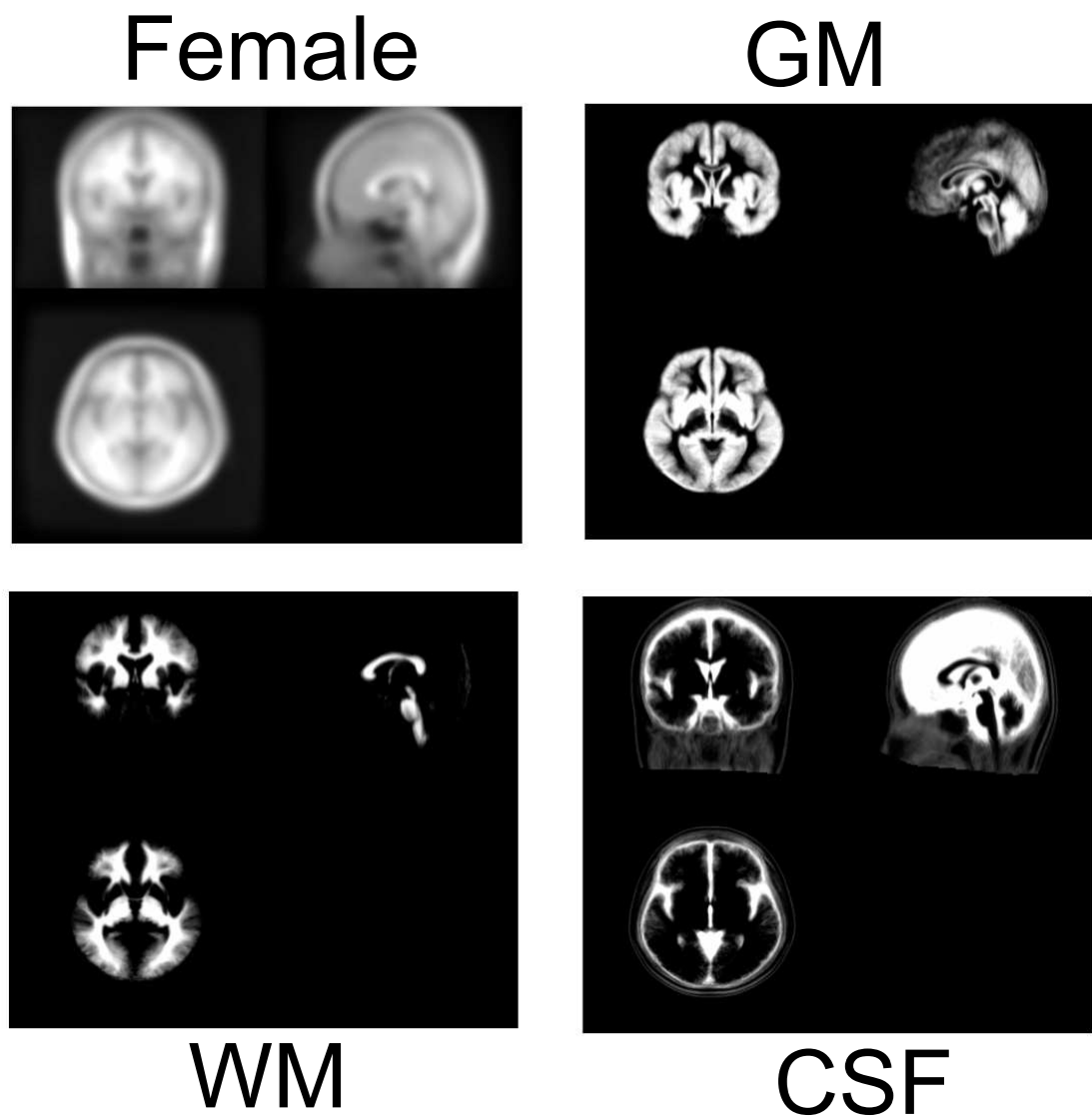
Figure 4.6: **Taiwanese Female Template.** 30 normal female adult subjects were taken to construct Taiwanese brain template by our proposed method. Age range is from 18 to 35 years old (22.9 ± 4.6264).

4.3.2 Tissue Probability Maps

Brain tissue could be classified into three different types, gray matter (GM), white matter (WM) and cerebral spinal fluid (CSF). Segmentation and volume measurements of these three tissue types on MRI is an important issue on clinical and medical researches. Therefore, we have also constructed GM, WM and CSF tissue probability templates of Taiwanese by the following steps.

1. Segmentation

    (a) Normalize each individual brain into ICBM152 space.

    (b) Segment each individual brain into three tissue classes (GM, WM, CSF) according to ICBM apriori tissue probability maps.

    (c) Normalize three segmented brains of each individual brain back to its original space.

2. Normalize each individual brain to Taiwanese template and obtain a transformation matrix.

3. Normalize every individual segmented brain by its transformation matrix in step 2.

4. Average all these transformed segmented brain volumes of the same tissue class and finally form templates of three tissue classes.

Segmentation and normalization were done by statistical parametric mapping (SPM, Wellcome Department of Imaging Neuroscience, UK, http://www.fil.ion.ucl.ac.uk/spm/)[8], which is a MATLAB (The Math Works, Inc., Natick, MA, USA) software package.
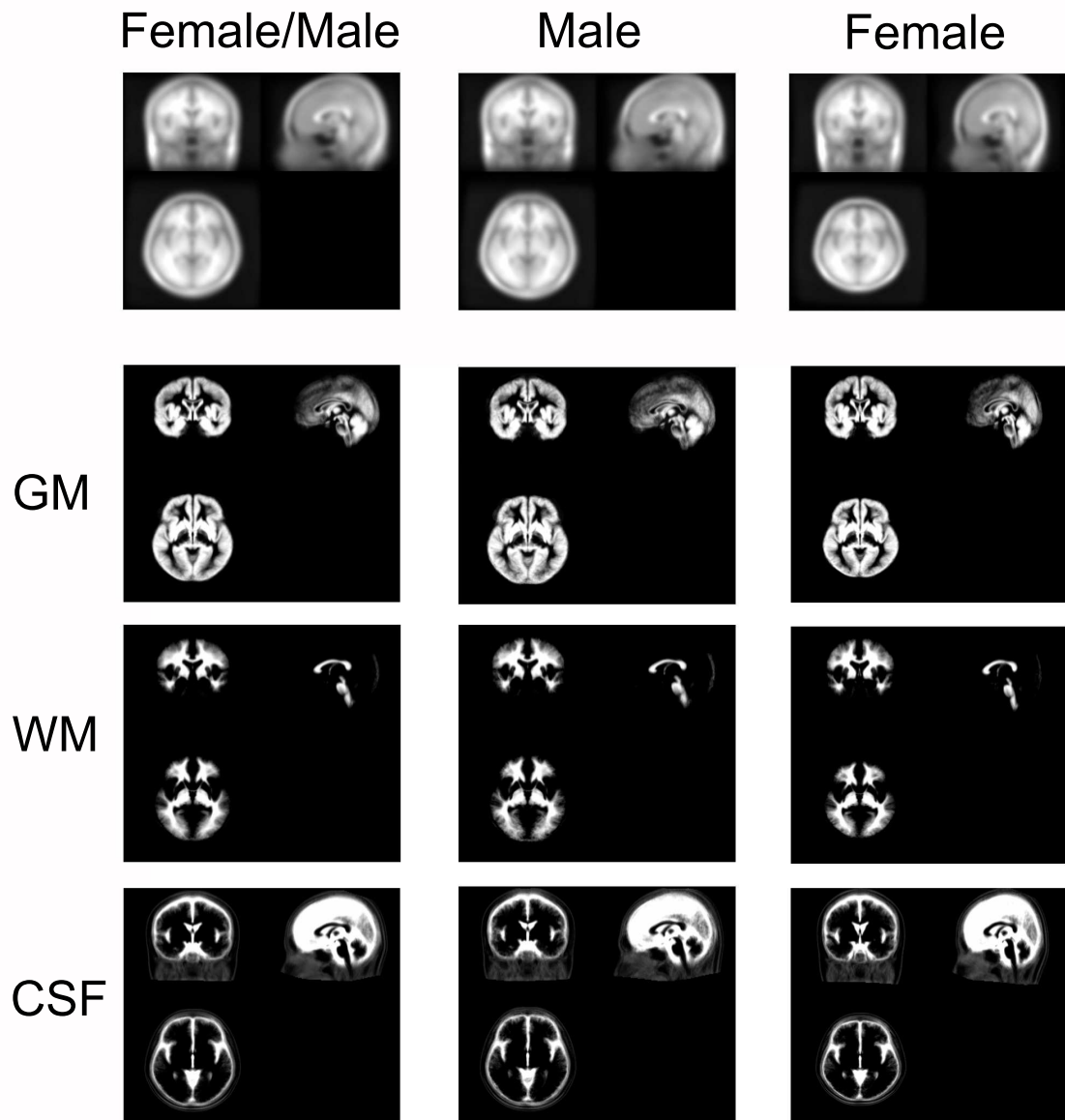
Figure 4.7: **Taiwanese Templates.** The first row are intensity average brain atlas which constructed by our method described in previous chapters. The other rows are gray matter (GM), white matter (WM) and cerebral spinal fluid (CSF) templates for both gender, male and female in order. These tissue probability maps were constructed by normalizing each segmented brain to template space and averaging these transformed segmented brain of same tissue class.

4.3.3 Brain Mask

A template brain mask could separate brain cortex from head MRIs in order to ignore skull and background intensities. Segmentation, normalization or some other analysis progresses may apply a brain mask to remove non-cortical structures. There are many ways for brain mask construction. We have tried the following methods.

1. Manually ROI selection

2. A software package : Brain Extraction Tool (BET [34])

3. Build by piling up GM, WM and CSF templates

Method 1 is so laborious and not a precise way to extract cortex. In method 2, BET is a software library maintained by FMRIB Image Analysis Group (http://www.fmrib.ox.ac.uk /analysis/research/bet/) [34]. A free software which used to display brain volume, MRIcro (http://web.arizona.edu/ cnl/mricro.htm), has contained this library in its application. There is a parameter needed to regulate for BET doing the skull striping in MRIcro. However, we could only tune up an acceptable value for this parameter which usually also leave some residual skull, just like figure 4.8 shows. Therefore, manually ROI selection was done in order to clean up skull.

Another brain mask construction method is based on GM, WM and CSF brain templates. Voxel value in GM, WM and CSF template means the probability of tissue type. By piling up these three tissue probability maps, a pure cortex volume was obtained. The voxel value in this pure cortex volume means the probability to be one of these three tissue types. We decide a threshold and cut off values lower than threshold. Figure 4.9 show the brain masks with different thresholds.
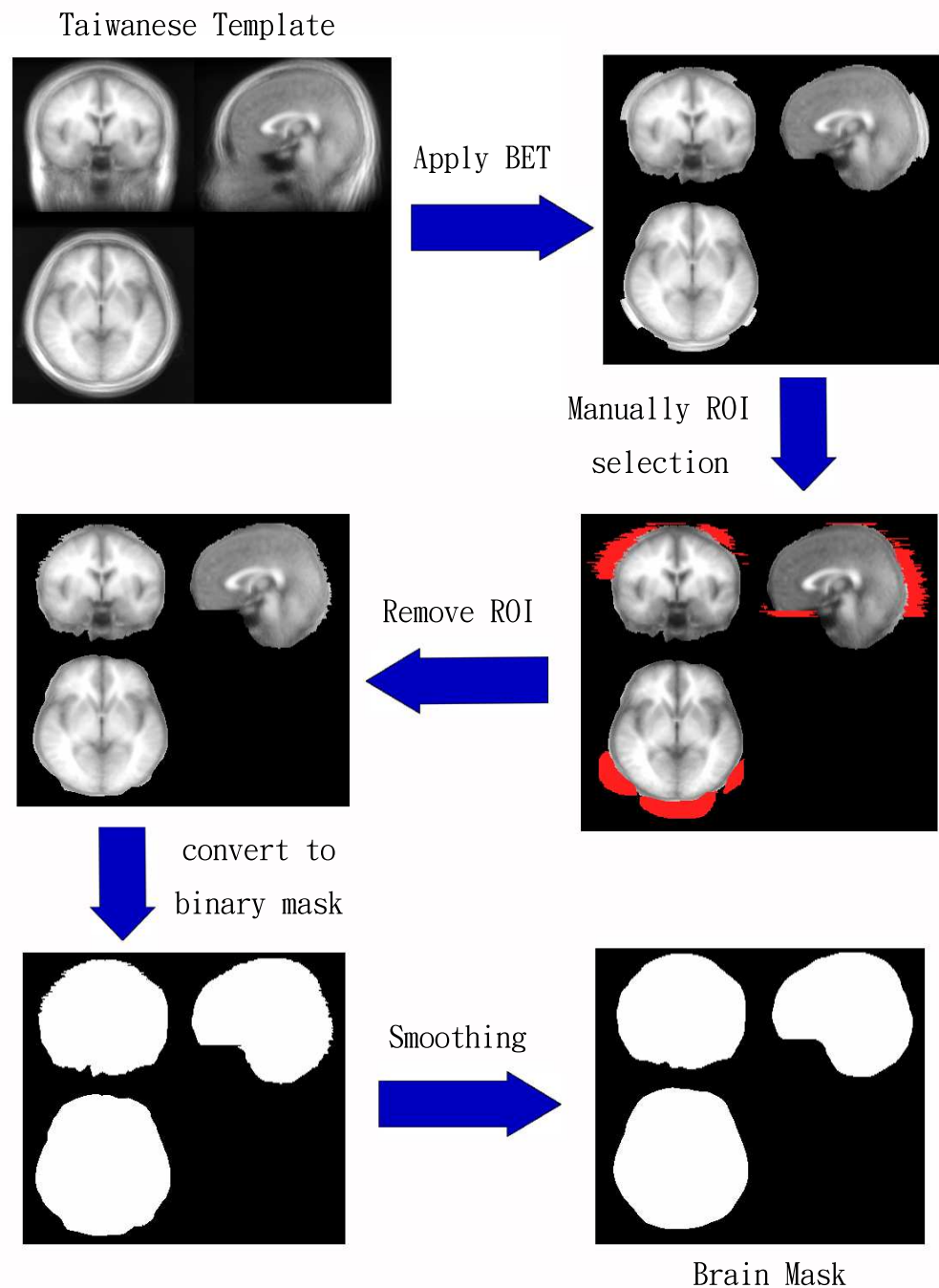
Figure 4.8: **Brain Mask build by BET and manually ROI selection.** We first use BET to extract cortex by regulating a parameter. However, we could only tune up an acceptable value for this parameter which usually also leave some residual skull. Therefore, manually ROI selection was done in order to clean up skull.

threshold = 0

threshold = 0.30

threshold = 0.45

threshold = 0.65
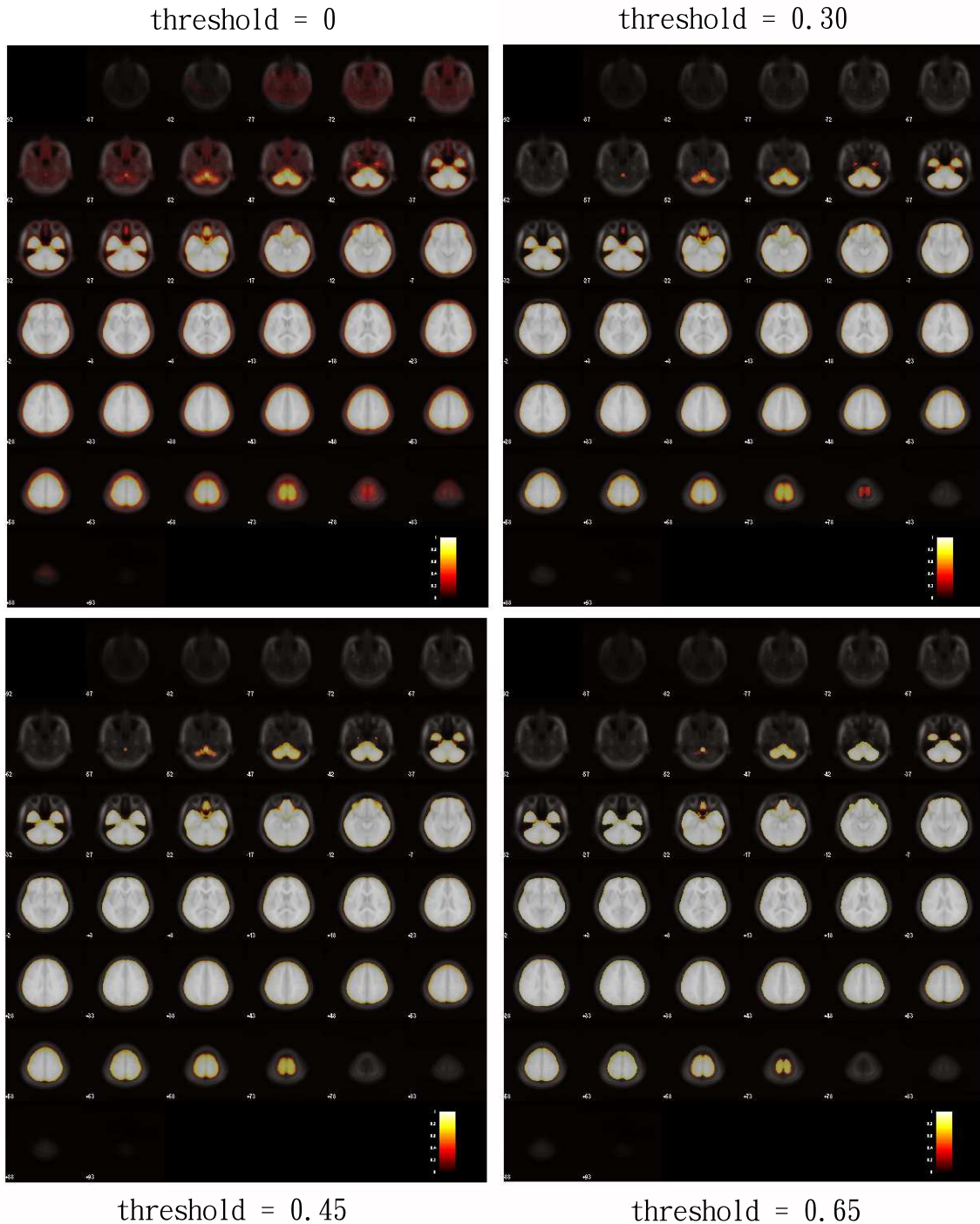
Figure 4.9: **Taiwanese template brain masks.** Brain mask construction method described here is based on GM, WM and CSF brain templates. Voxel value in GM, WM and CSF template means the probability of tissue type. By piling up these three tissue probability maps, a pure cortex volume was obtained. The voxel value in this pure cortex volume means the probability to be one of these three tissue types. We decide a threshold and cut off the lower values. In this figure show the brain masks with different thresholds.

4.4 Experiments on Taiwanese Template

4.4.1 Ratio of Gray Matter to White Matter

Ratio of gray matter to white matter, said "gray-white ratio", is also an important issue for measurement of brain volume. Gray-white ratio was said to be stable over the age and seemed no difference on sex[9]. We calculated gray-white ratio by the following steps.

1. Segmentation

   (a) Normalize each individual brain into Taiwanese brain template space.

   (b) Segment each individual brain into three tissue classes (GM, WM, CSF) according to Taiwanese tissue probability maps.

   (c) Normalize three segmented brains of each individual brain back to its original space.

2. Multiply voxel value (probability of tissue type) by voxel volume. The resulting value is volume of tissue type.

3. Calculate ratio of gray matter volume to white matter volume.

Table 4.3 lists calculated values. Volume of gray matter for 58 subjects is 0.5895 ± 0.0639 liter, for female is 0.5715 ± 0.0631 liter and for male is 0.6089 ± 0.0600 liter, respectively. Volume of white matter for 58 subjects is 0.3958 ± 0.0434 liter, for female is 0.3737 ± 0.0339 liter and for male is 0.4194 ± 0.0402 liter, respectively. Gray-white matter ratio for 58 subjects is 1.4937 ± 0.1058, for female is 1.5297 ± 0.0986 and for male is 1.4552 ± 0.1011, respectively. The measured gray-white matter ratios represented stable values on each individual brain, which means there were no significant variability of gray-white matter ratio on normal brains, just as Gea et al. [9] stated.

	All subjects		Female subjects		Male subjects	
Measurement	Mean	Std.	Mean	Std.	Mean	Std.
Gray Matter Volume (l.)	0.5895	0.0639	0.5715	0.0631	0.6089	0.0600
White Matter Volume (l.)	0.3958	0.0434	0.3737	0.0339	0.4194	0.0402
Gray-White Ratio	1.4937	0.1058	1.5297	0.0986	1.4552	0.1011

Table 4.3: **Tissue volumes of Taiwanese Template by being segmented according to Taiwanese apriori tissue probability maps.**

Compared to other researches, Kim et al. [18] measured gray-white matter ratio on Korean template was 1.36 and on ICBM 452 template was 1.30 [20]. For Allen et al. [1]'s study, the gray-white matter ratio of women is 1.35 compared with 1.26 of men. And for Gea et al. [9], they claimed value of gray-white matter ratio for women is 1.4 and for men is 1.5. Therefore, measured values of gray-white matter ratio on Taiwanese template were distributed in a reasonable range.

There have been two factors claimed to affect value of gray-white matter ratio, which are image brightness and segmentation method.

1. **Brightness**

   Harris et al. [12] said that the brighter images seemed to let segmentation more overestimate the gray matter. On the other hand, the dimmer images seemed to let segmentation more underestimate the gray matter.
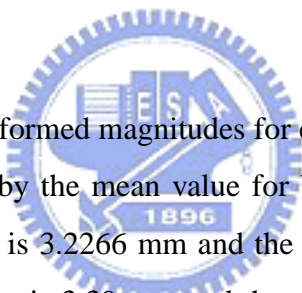
2. **Segmentation Method**

   Schaper et al. [32] compared seven different automated tissue segmentation packages to observe outcome of gray-white matter ratio. Among these methods, five packages (FAST, SEGM, FANTASM, PVS, PVE) obtained ratio values distributed between 1.1 to 1.5 and the other two packages (INSECT, SPM) produced higher values, 1.5 to

2.0, on gray-white matter ratio for the same brain MRI volumes. To our significant concern, SPM was indicted notably tends to overestimate the gray-white matter ratio. They suggested that it might caused by SPM put reliance on the alignment to the template contour.

In a conclusion, by observing the measured gray matter and white matter tissue volumes, two factors described above may biased to overestimate gray-white matter ratio.

4.4.2   Deformation Field from Individual Brains to Taiwanese Template

We calculate sum of deformed magnitudes for every individual brain normalize to Taiwanese template and sort by the mean value for both gender groups (figure 4.10). The mean value of male group is 3.2266 mm and the standard deviation is 0.2376 mm. The mean value of female group is 3.39 mm and the standard deviation is 0.3242 mm. It reveals that male group is more close to the Taiwanese template. A reasonable suggestion is that the representative brain of Male group is the same as of both gender groups.

4.4.3   Distribution of Regional Deformation Variation

By observing distribution of regional deformation variation, we could know the variable regions of individual brain. Method to reveal distribution of regional deformation variation is as follows, deformation field from every individual brain to Taiwanese template was recorded. Then we averaged magnitude of deformation field on the same voxel of each brain. Finally, a brain volume that its voxel value represents mean or standard deviation value of magnitude on the same voxel was formed. The more variable region would represent the higher value.
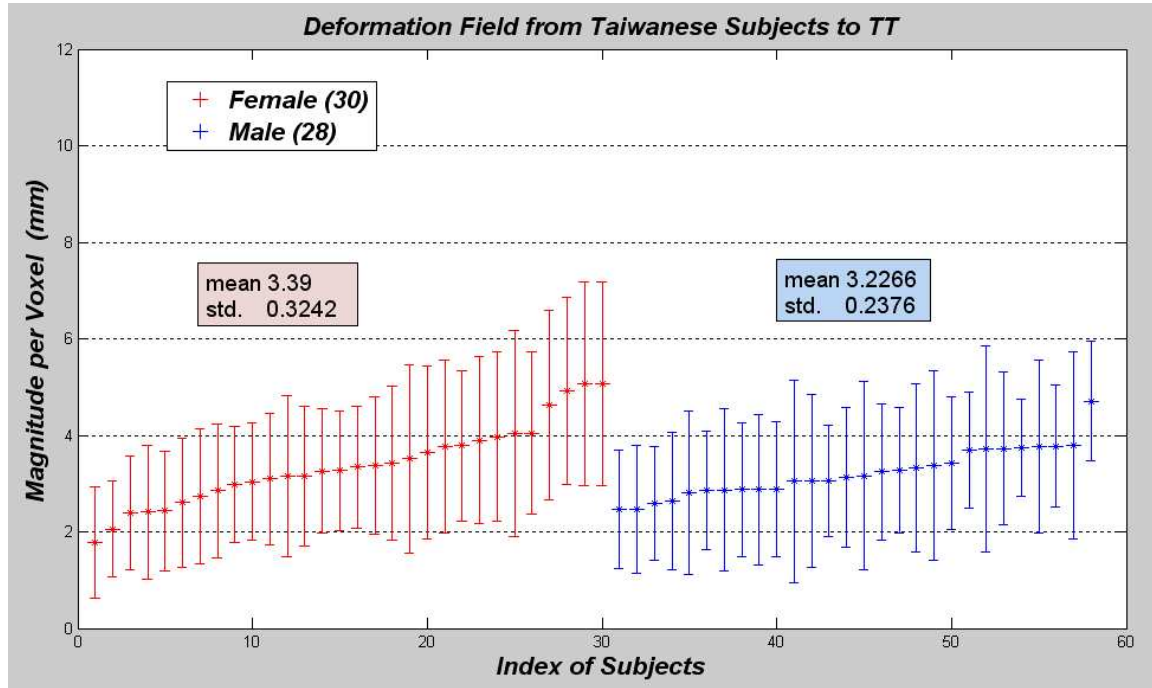
Figure 4.10: **Deformation field from individual brains to Taiwanese template.** We calculate sum of deformed magnitudes for every individual brain normalize to Taiwanese template and sort by the mean value for both gender groups. The mean value of male group is 3.2266 mm and the standard deviation is 0.2376 mm. The mean value of female group is 3.39 mm and the standard deviation is 0.3242 mm.

As figure 5.8 shows, the most significant variable region is cerebellum. The second significant variable region is appeared on part of parietal lobe. The more inside the brain cortex represents a stable similarity of every individual brain.
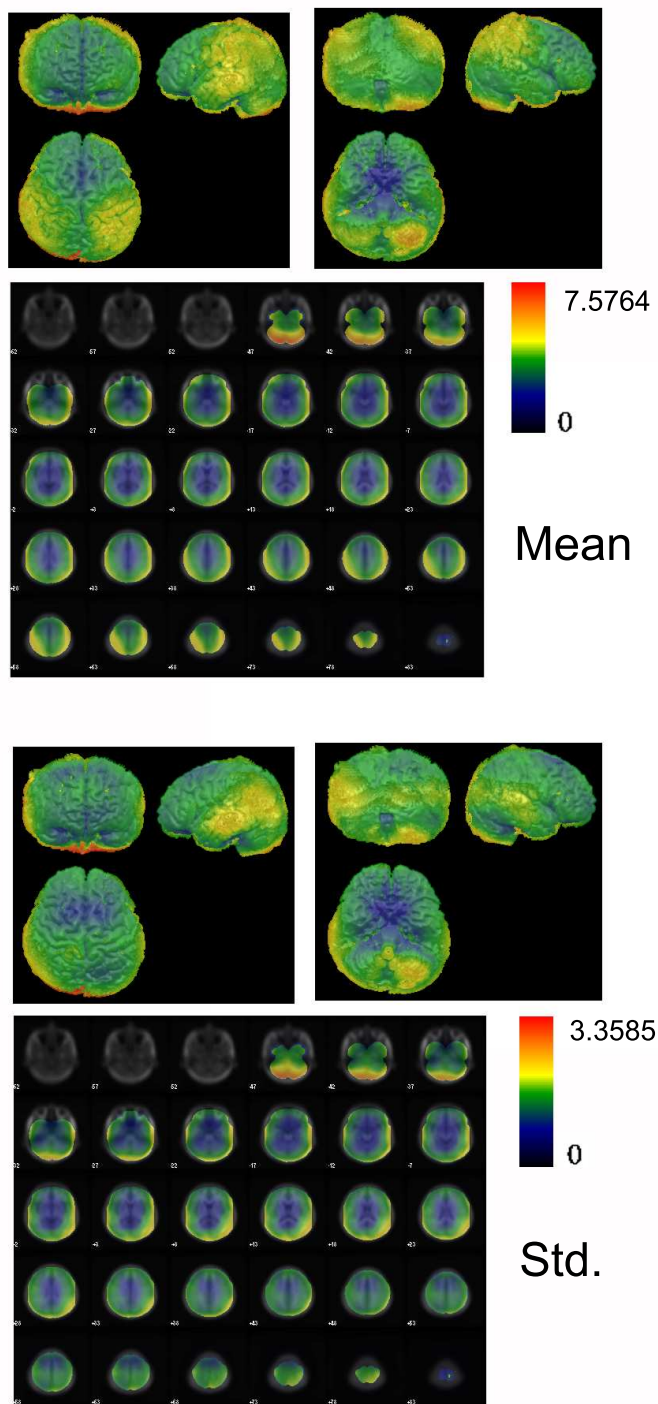
Figure 4.11: **Distribution of regional variation from Taiwanese subjects to Taiwanese template.** In order to realize the variable regions of individual brain, deformation field from every individual brain to Taiwanese template was recorded. We averaged magnitude of deformation field on the same voxel of each brain. Then, a brain volume that its voxel value experiments mean or standard deviation value of magnitude on the same voxel was formed. The more variable region would represent the higher value.

Chapter 5

Discussion

5.1 Comparison of Different Ethnic Groups

In this section, we list several comparison between brain templates. Among these brain templates, Talairach brain, MNI305, ICBM152 and ICBM452 were build up from Western people. On the other hand, Korean100 and Taiwanese58 were build up from Eastern people. For a global view of these comparison, ethnic difference of brain volume indeed exists. And the results reveal that Taiwanese template is shorter and wider than the Western template. Accompanied with results of Zilles et al. [43] and Kim et al. [18], we may conjecture that brain volumes of the Eastern people are shorter and wider than the Western people's.

5.1.1 Ratio of Maximum Length to Maximum Width of Brain Templates

Ratio of maximum length to maximum width reveals the global characteristic of brain shape. For the definition of the maximum width as well as the maximum length, these two measurements were defined on the slice that reveals AC-PC line as the middle line. Additionally, the maximum length is the distance from the most anterior cortex to the most posterior cortex and the maximum width is the distance from the leftest cortex to the rightest cortex.

Figure 5.1 and table 5.1 list maximum length to maximum width ratio of every brain template. Talairach brain has the maximum value of ratio, 1.31544. Ratio of MNI305, ICBM152, ICBM452, Korean100 and Taiwanese58 are 1.2638, 1.2638, 1.2794, 1.1511 and 1.0811, respectively. It is clear to see that both templates of Eastern people (Korean100, Taiwanese58) are shorter in anterior-to-posterior length and wider in left-to-right width than of Western people (Talairach brain, MNI305, ICBM152, ICBM452). In another way, for the Eastern part, length of Korean template is almost the same as Taiwanese template, but width of Korean template is a little shorter than the Taiwanese template.
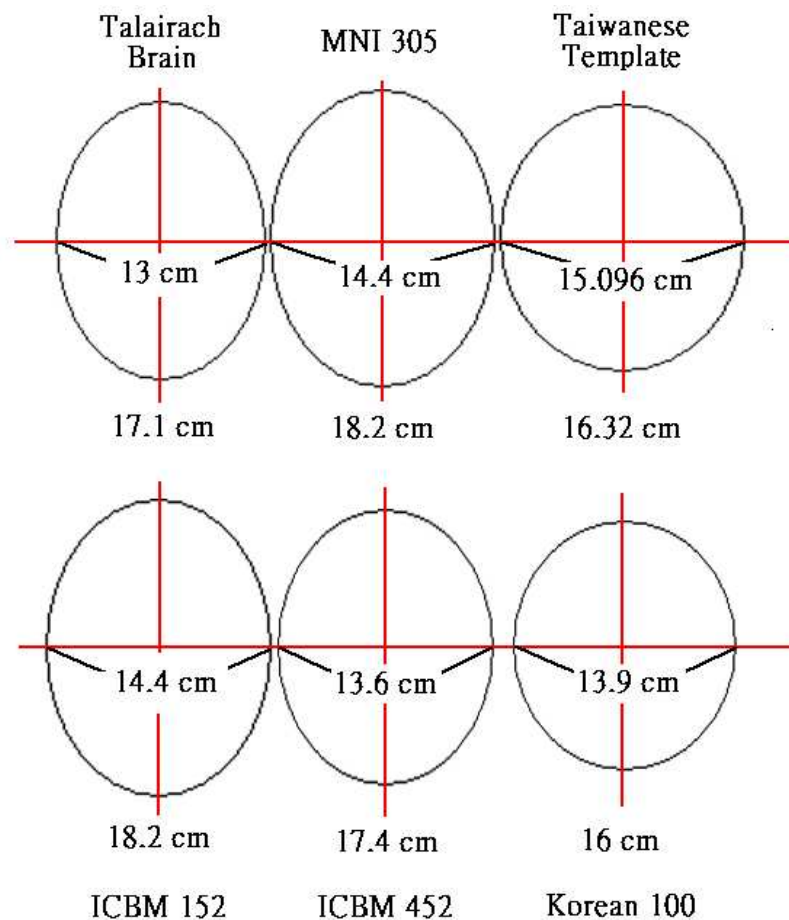
Figure 5.1: **Ratio of maximum length and maximum width of brain templates.** A measurement of global brain shape characteristic is to estimate the maximum length and maximum width of brain volumes. Here we defined the maximum length as the distance from the most anterior cortex to the most posterior cortex on the slice that reveals AC-PC line as the middle line. Besides, the maximum width was defined as the distance from the leftest cortex to the rightest cortex on the slice that reveals AC-PC line as the middle line.

	Templates					
	Talairach	MNI 305	ICBM 152	ICBM 452	Korean 100	Taiwanese 58
Length(cm)	17.1	18.2	18.2	17.4	16	16.32
Width(cm)	13	14.4	14.4	13.6	13.9	15.096
$\frac{Length}{Width}$	1.31544	1.2638	1.2638	1.2794	1.1511	1.0811

Table 5.1: **Ratio of maximum width to maximum length of brain templates.**

Ratio of Gray Matter to White Matter

Gea et al. [9] claimed that gray-white matter ratio only altered slightly within the age of 20-86 years old. Besides, there was no significant effects on sex. Referring to other researches, Kim et al. [18] measured gray-white matter ratio on Korean template and ICBM 452 were 1.36 and 1.30, respectively [20]. For Allen et al. [1]'s study, the gray-white matter ratio of women is 1.35 compared with 1.26 of men. And for Gea et al. [9], they claimed value of gray-white matter ratio for women is 1.4 and for men is 1.5.

In our studies, we segmented every individual brain into GM, WM and CSF in Taiwanese template space by SPM and finally calculated volumes of these three tissue types. The resulting gray-white matter ratio was 1.4937 ± 0.1058, for female is 1.5297 ± 0.0986 and for male is 1.4552 ± 0.1011, respectively (table 4.3). These values were stable for all subjects and distributed in a reasonable range.

Here we tempted to segment individual brains in ICBM152 space on the purpose to see if it is more reasonable when doing segmentation in Taiwanese template space then in ICBM152 space. Table 5.2 lists calculated values. Volume of gray matter for 58 subjects is 0.7823 ± 0.0802 liter, for female is 0.7467 ± 0.0669 liter and for male is 0.8205 ± 0.0765 liter, respectively. Volume of white matter for 58 subjects is 0.4016 ± 0.0446 liter, for

female is 0.3766 ± 0.0317 liter and for male is 0.4283 ± 0.0411 liter, respectively. Gray-white ratio for 58 subjects is 1.9521 ± 0.0903, for female is 1.9836 ± 0.0828 and for male is 1.9184 ± 0.0871, respectively. Although Gray-white matter ratio values were also stable for all subjects, the calculated gray matter volume seemed too large and lead to a unreasonable high gray-white matter ratio.

	All subjects		Female subjects		Male subjects	
Measurement	Mean	Std.	Mean	Std.	Mean	Std.
Gray Matter Volume (l.)	0.7823	0.0802	0.7467	0.0669	0.8205	0.0765
White Matter Volume (l.)	0.4016	0.0446	0.3766	0.0317	0.4283	0.0411
Gray-White Ratio	1.9521	0.0903	1.9836	0.0828	1.9184	0.0871

Table 5.2: **Tissue volumes of Taiwanese Template by being segmented according to ICBM apriori tissue probability maps.**
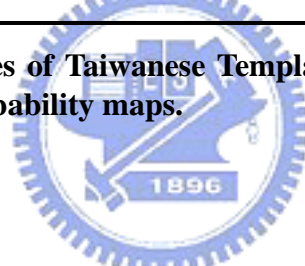
5.1.2 Deformation Field between Templates

In order to find out the diversity of Western brain and Eastern brain, we observed the difference between ICBM templates and Taiwanese template. Figure 5.3, Figure 5.4 and Figure 5.5 show the magnitude of deformation field when doing the normalization between MNI305 (a template with skull) and Taiwanese template (with skull), ICBM152 (a template with skull) and Taiwanese template (with skull) and ICBM452 (a template without skull) and Taiwanese template (without skull), respectively. A deformation toolbox of statistical parametric mapping (SPM, Wellcome Department of Imaging Neuroscience, UK, http://www.fil.ion.ucl.ac.uk/spm/)[8], which is a MATLAB (The Math Works, Inc., Natick, MA, USA) software package, was used to estimate the deformation field of normalization.

For calculating magnitude of deformation field, following lists the steps that we had processed :

1. Calculating deformation field with normalization matrix by SPM deformation tool-
   box.

2. Removing effects of pose and size by SPM deformation toolbox.

3. Calculation magnitude from deformation field.

Because of step 2., the deformation field here represents only effect of brain shape. There
is no matter about the brain size and pose.

A parameter, named "defaults.normalise.estimate.reg", was adjusted to bring up a fine
normalization. This parameter is about the ratio of deformation smoothness and deforma-
tion freedom. Additionally, the default value in SPM is 1. The larger the value means to
take more account on deformation smoothness and the resulting normalized volume would
be more similar to the original brain volume. Magnitude of deformation field with different
values of "defaults.normalise.estimate.reg" are listed in tables for different brain templates
(table numbers are 5.3, 5.4, 5.5, 5.6, 5.7 and 5.8).

MNI305 v.s. Taiwanese template

For normalization between MNI305 and Taiwanese template, there was no proper value
of "defaults.normalise.estimate.reg" to form a reasonable and fine result. Especially, weird
warping results appeared while parameter "defaults.normalise.estimate.reg" was set as 0.1
and 0.01. As figure 5.2 shows, top of cortex was warped extending out of the skull. A
conjecture for the bad warping results was that the volume of template MNI305 was skull-
scraped on top and the first stage of SPM normalization is based on the skull.

We took a tolerable warping result for discussion and that was the result of setting "de-
faults.normalise.estimate.reg" as 10, as figure 5.3 shows. For a global view on it, either the
warping direction is from MNI305 to Taiwanese template or the direction from Taiwanese

template to MNI305, large values of magnitude are surround the surface of brain. The more inside the brain, the warping magnitude is decayed. For a detailed view on it, as the warping direction is from MNI305 to Taiwanese template, deformation field on top and bottom of the brain region seems larger than the reverse direction.

defaults.normalise. estimate.reg	max (mm)	mean (mm)	std. (mm)
0.01	43.4283	8.4288	9.2601
0.1	20.0225	4.0247	4.0916
1	9.673	3.0369	2.9287
10	9.0284	3.1991	2.9598
100	8.5732	3.1047	2.8704

Table 5.3: **Magnitude of deformation field from MNI305 to Taiwanese template.**

defaults.normalise. estimate.reg	max (mm)	mean (mm)	std. (mm)
0.01	89.0722	14.352	14.9527
0.1	51.6435	8.6088	9.5740
1	18.8916	3.7343	3.5235
10	7.9765	3.0042	2.5902
100	8.4032	3.0402	2.5931

Table 5.4: **Magnitude of deformation field from Taiwanese template to MNI305.**
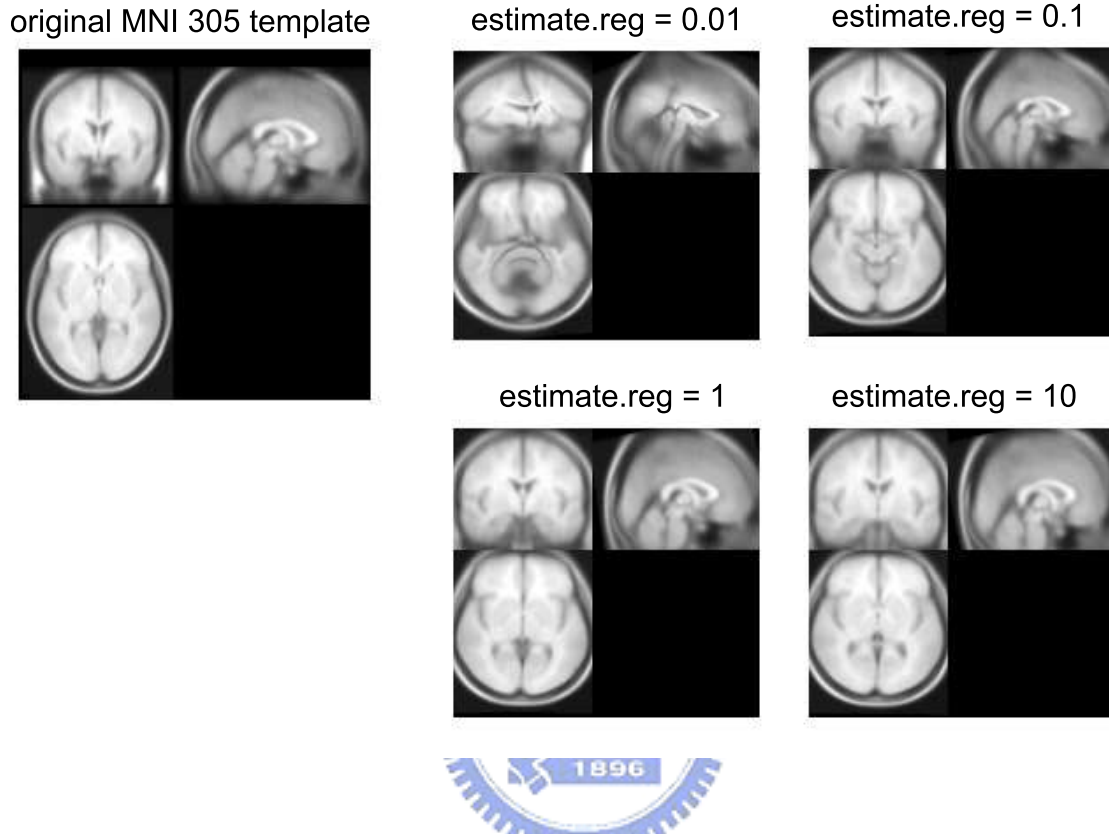
Figure 5.2: **Warping results from MNI305 to Taiwanese template with different parameters.** (left) The original MNI305 brain template which is skull-scraped on top of cortex. (right) Warping results as defaults.normalise.estimate.reg was set as 0.01, 0.1, 1 and 10, respectively. Taking observation on the parameter which was set as 0.01 and 1, it appeared weird warping results. We can see that the top of cortex was extended out of the skull.

ICBM152 v.s. Taiwanese template

Another case of Western template, ICBM152, was took as comparison as well. Figure 5.4 shows the magnitude of deformation field of both directions and the parameter "defaults.normalise.estimate.reg" was set as 10. Unlike MNI305, the original ICBM152 template has a complete skull around the brain cortex. Therefore, either the normalization from ICBM152 to Taiwanese template or the normalization from Taiwanese template to ICBM152, warping variation seems good and symmetrical in both directions.
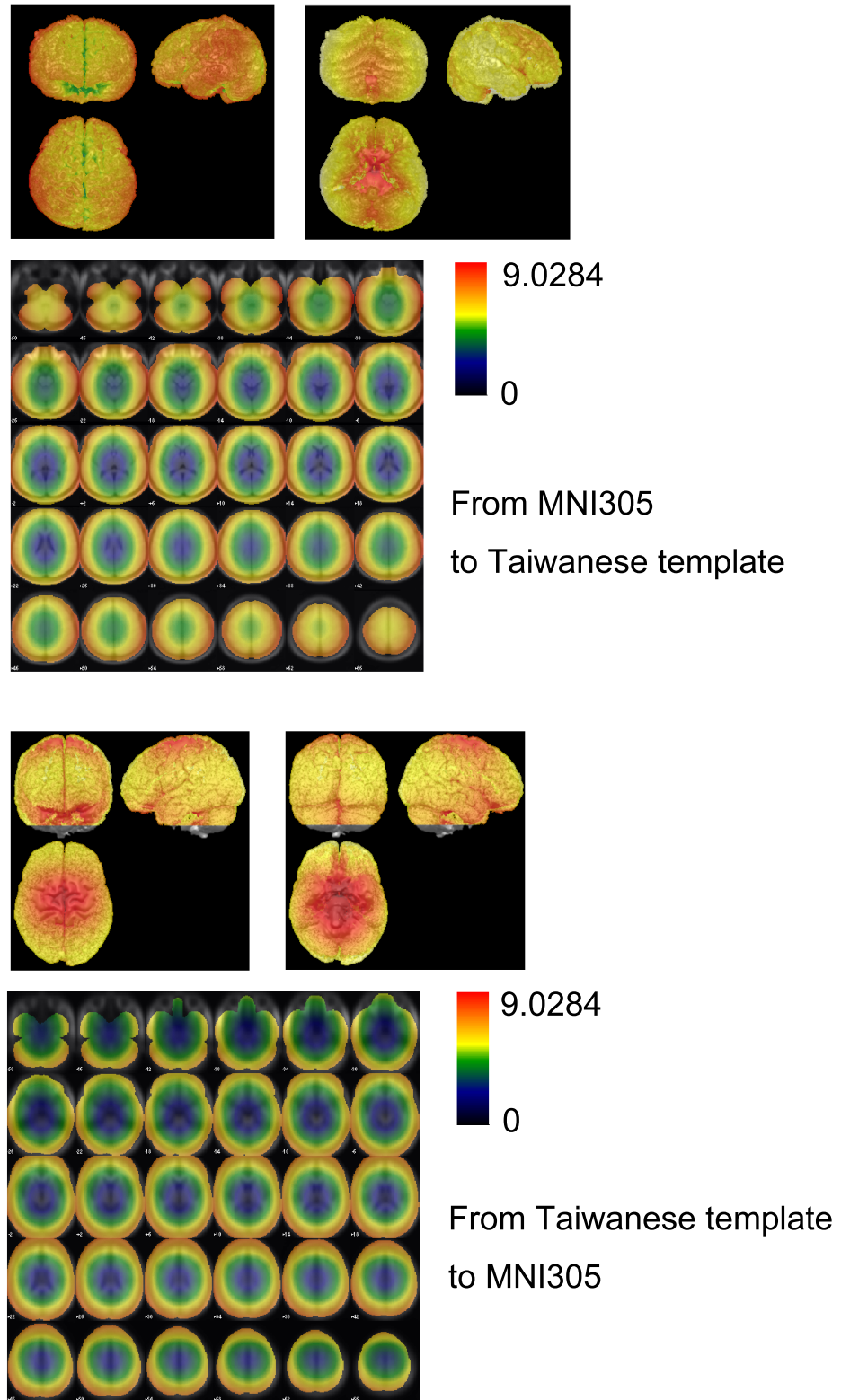
From MNI305
to Taiwanese template

From Taiwanese template
to MNI305

Figure 5.3: **Magnitude Dif deformation field between MNI305 and Taiwanese template with defaults.normalise.estimate.reg = 10.**

For a more detailed view, the deformation field only reveals large values on the top, bottom and lateral sides of brain surface, excluding frontal and occipital lobes. Because we have known that Taiwanese template is shorter and wider than ICBM152, it seems reasonable if the frontal and occipital lobe have large value of magnitude of deformation field. On our guess, it may caused by the step of calculating deformation field which has already contained removing effect of brain pose and size. Thus, the resulting deformation field leaves only effect of brain shape. As the result, if the procedure of removing size fixed anterior to posterior length on brain, the brain shape difference would significantly exhibit on top, bottom and lateral sides.

ICBM452 v.s. Taiwanese template

Furthermore, ICBM452, a Western template without skull, was took for comparison as well. For a reciprocal normalization between ICBM452 and Taiwanese template, a skull-strip procedure was done on the Taiwanese template to form a Taiwanese template without skull. Then we took these two templates without skull for normalization.

ICBM452 and Taiwanese template is the only pair that values of mean standard deviation on magnitude of deformation field represent nearly the same, which perform a pretty result. However, taking a view of the deformation field, distribution of warping variation looks not so similar with each other. Both of warping directions appears large values on lateral sides and occipital lobes. But deformation field of normalization from Taiwanese template to ICBM452 additionally reveals large magnitude on frontal lobe where from the inverse direction it reveals small magnitude.

defaults.normalise. estimate.reg	max (mm)	mean (mm)	std. (mm)
1	10.7592	2.5452	2.9520
10	9.8056	2.4435	2.8774
50	9.6851	2.4129	2.8473

Table 5.5: **Magnitude of deformation field from ICBM152 to Taiwanese template.**

defaults.normalise. estimate.reg	max (mm)	mean (mm)	std. (mm)
1	17.4574	4.3193	3.9642
10	11.0105	3.5958	3.1405
50	9.8419	3.52	3.0666

Table 5.6: **Magnitude of deformation field from Taiwanese template to ICBM152.**

From ICBM 152

 to Taiwanese template

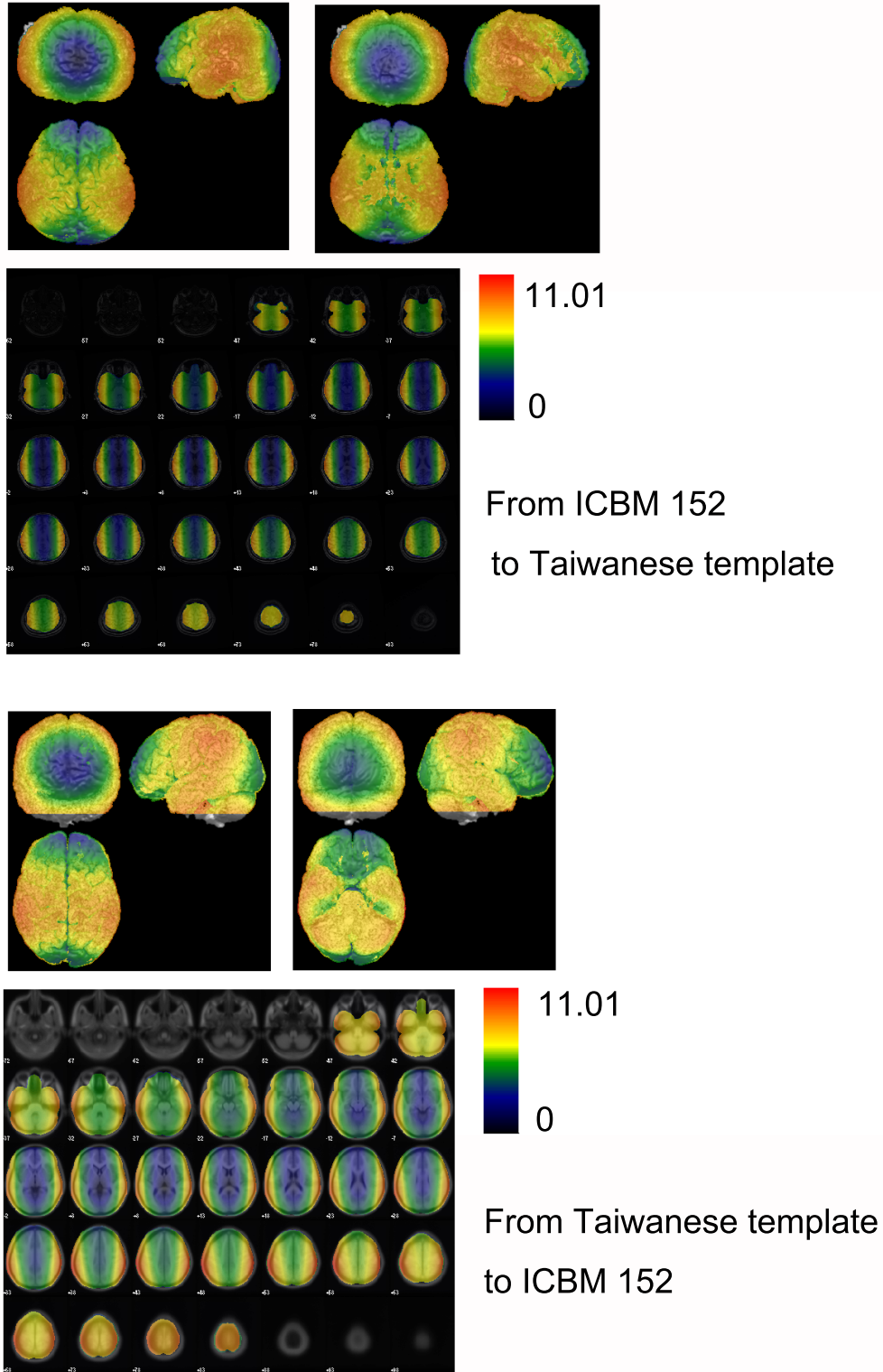From Taiwanese template

to ICBM 152

Figure 5.4: **Magnitude of deformation field between ICBM152 and Taiwanese template with defaults.normalise.estimate.reg = 10.**

defaults.normalise. estimate.reg	max (mm)	mean (mm)	std. (mm)
1	9.3979	2.1711	2.5510
10	8.5301	2.1432	2.5116

Table 5.7: **Magnitude of deformation field from ICBM452 to Taiwanese template.**

defaults.normalise. estimate.reg	max (mm)	mean (mm)	std. (mm)
1	11.0465	2.3945	2.8093
10	9.5398	2.215	2.654

Table 5.8: **Magnitude of deformation field from Taiwanese template to ICBM452.**
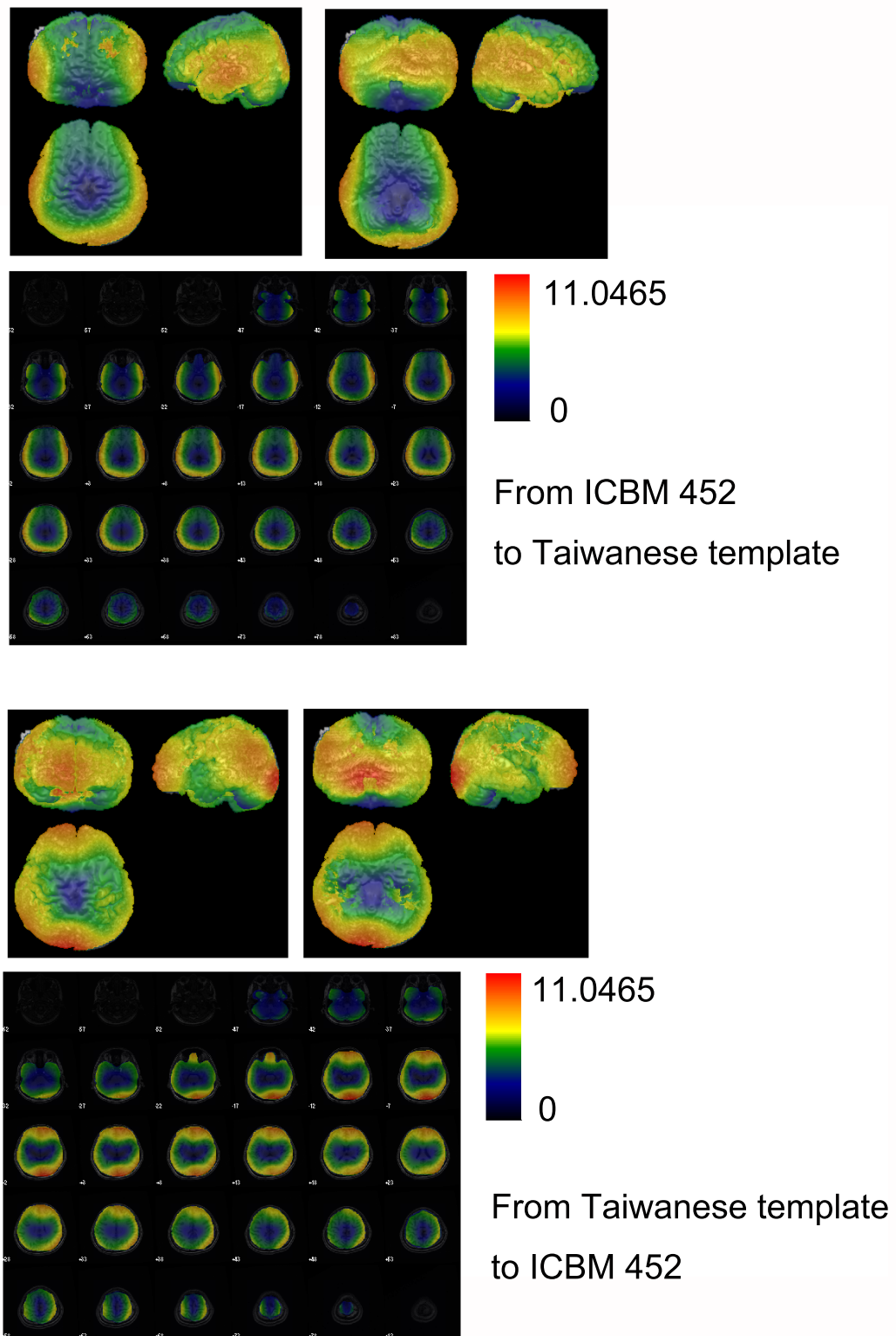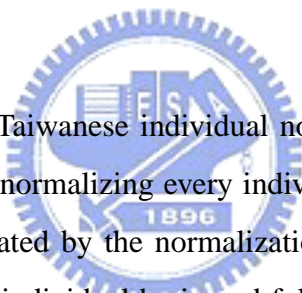
Figure 5.5: **Magnitude of deformation field between ICBM452 and Taiwanese template with defaults.normalise.estimate.reg = 1.**

5.1.3   Deformation Field from Individual Brains to Templates

A good template should make distortion of normalization as little as possible. Magnitude of deformation field is a kind of measurement to represent the distortion. Figure 5.6 shows the mean magnitude per voxel of each individual volume while normalizing to templates, Taiwanese template, MNI305 and ICBM152, respectively. It is a significant evidence that a template constructed from Taiwanese could diminish the distortion of Taiwanese volumes.

There were totally 58 Taiwanese individual normal brains, 30 for female and 28 for male, in our database. By normalizing every individual brain to a brain template, the deformation field was calculated by the normalization matrix. We averaged magnitude of deformation field for each individual brain and following the result, magnitude per voxel of an individual subject, was showed up in figure 5.6 for different templates.

Figure 5.6 (a) is for Taiwanese template (TT). The mean magnitude per voxel of every subjects is 3.31112, of female brains is 3.39 and of male brains is 3.2266. Figure 5.6 (b) is for template MNI305. The mean magnitude per voxel of every subjects is 5.12225, of female brains is 5.3016 and of male brains is 4.9301. Figure 5.6 (c) is for template ICBM152. The mean magnitude per voxel of every subjects is 5.51750, of female brains is 5.3777 and of male brains is 5.6673. There is no distinct difference between magnitude on deformation field of male and female. By integrating the above data, it is apparently that Taiwanese template stand more close to Taiwanese individual brain subjects, which means the Taiwanese template could cause a more accurate clinical analysis on Taiwanese cases by diminishing the distortion of normalization.
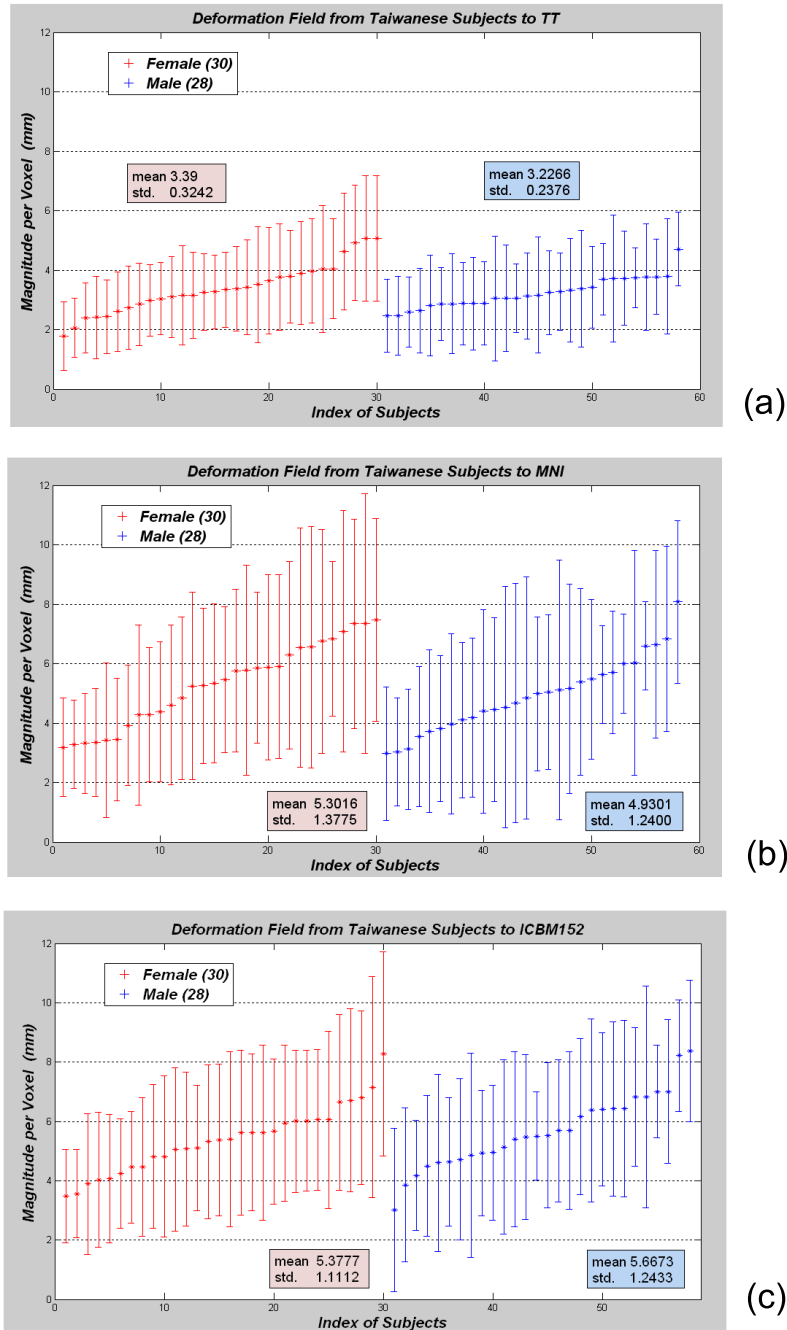
Figure 5.6: **Magnitude of deformation field from Taiwanese individual brain volumes to different templates.** For three brain templates (Taiwanese template, MNI305 and ICBM152), totally 58 Taiwanese individual brains (Female/Male : 30/28) were normalized to each of them. The resulting magnitude per voxel of deformation field for every individual brain were recorded in this figure. Obviously, deformation field of Taiwanese individual brains to Taiwanese template is smaller than to the other two Western templates (MNI305 and ICBM152), which means Taiwanese template could diminish the distortion of normalization for Taiwanese brain subjects.

5.1.4   Distribution of Regional Deformation Variation

Distribution of regional variation represents degree of variability on cortex of individual brains. While the calculation of deformation field from each individual brain to template were done, magnitude of deformation field on the same voxel of every brain subject were recorded. Then we calculate mean and standard deviation of the recorded values for every voxel. Finally, a brain volume which its voxel value represents mean or standard deviation value of magnitude on the same voxel was formed. The more variable region would represent the higher value. Here we took Taiwanese template, MNI305 and ICBM152 to observe the regional variation.

Figure 5.7 shows the brain that represents mean magnitude values of each voxel for normalizing to Taiwanese template (top), MNI305 (left) and ICBM152 (right). It is obviously that, for all voxels, the mean magnitude of Taiwanese individual brain subjects represent small values on the overall brain. That is to say, comparing to Western templates (MNI305 and ICBM152), Taiwanese template costs smallest value of normalization distortion for Taiwanese individual brains to be warped to it.

The distribution of regional variation as warping to Taiwanese template (figure 5.8), the significant variation is occurred on cerebellum. The second significant variable region is appeared on part of parietal lobe. On the other hand, when warping to MNI305 (figure 5.9), the most significant variable region is also the cerebellum and the second significant region is occipital lobe. In addition, when warping to ICBM152 (figure 5.10), the most significant variable region appear on parietal lobe and the cerebellum. For a conclusion of the above observation, the most variable region for warping is the cerebellum and parietal lobe.

Figure 5.7: **Distribution of regional variation from Taiwanese subjects to different templates.** We measured distribution of regional variation by averaging the magnitude of deformation field for every individual volumes on the same voxel. It is clear to see that the mean magnitude of every brain subjects are small for all voxels when the individual brain subject normalizes to Taiwanese template.
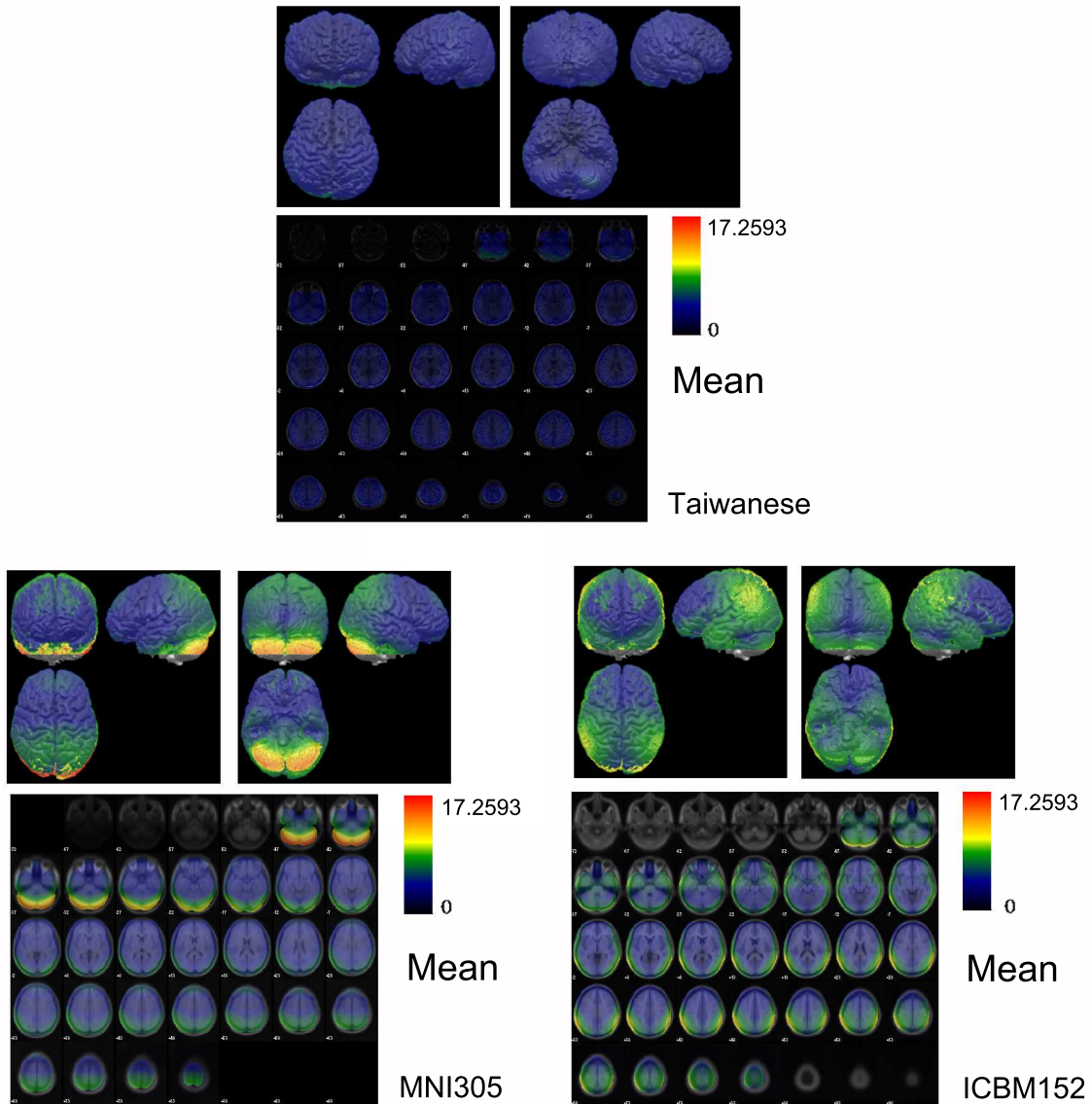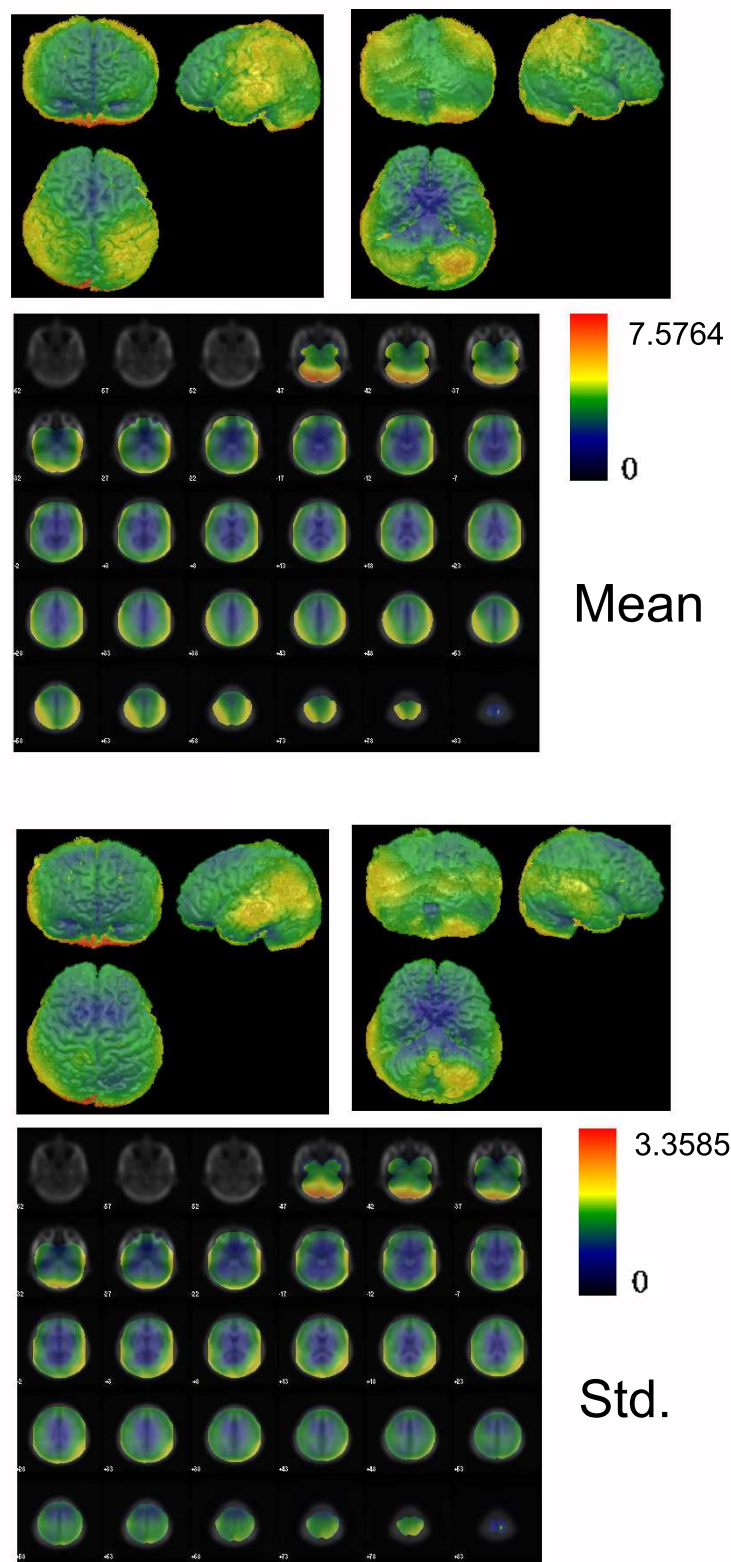
Figure 5.8: **Distribution of regional variation from Taiwanese subjects to Taiwanese template.**
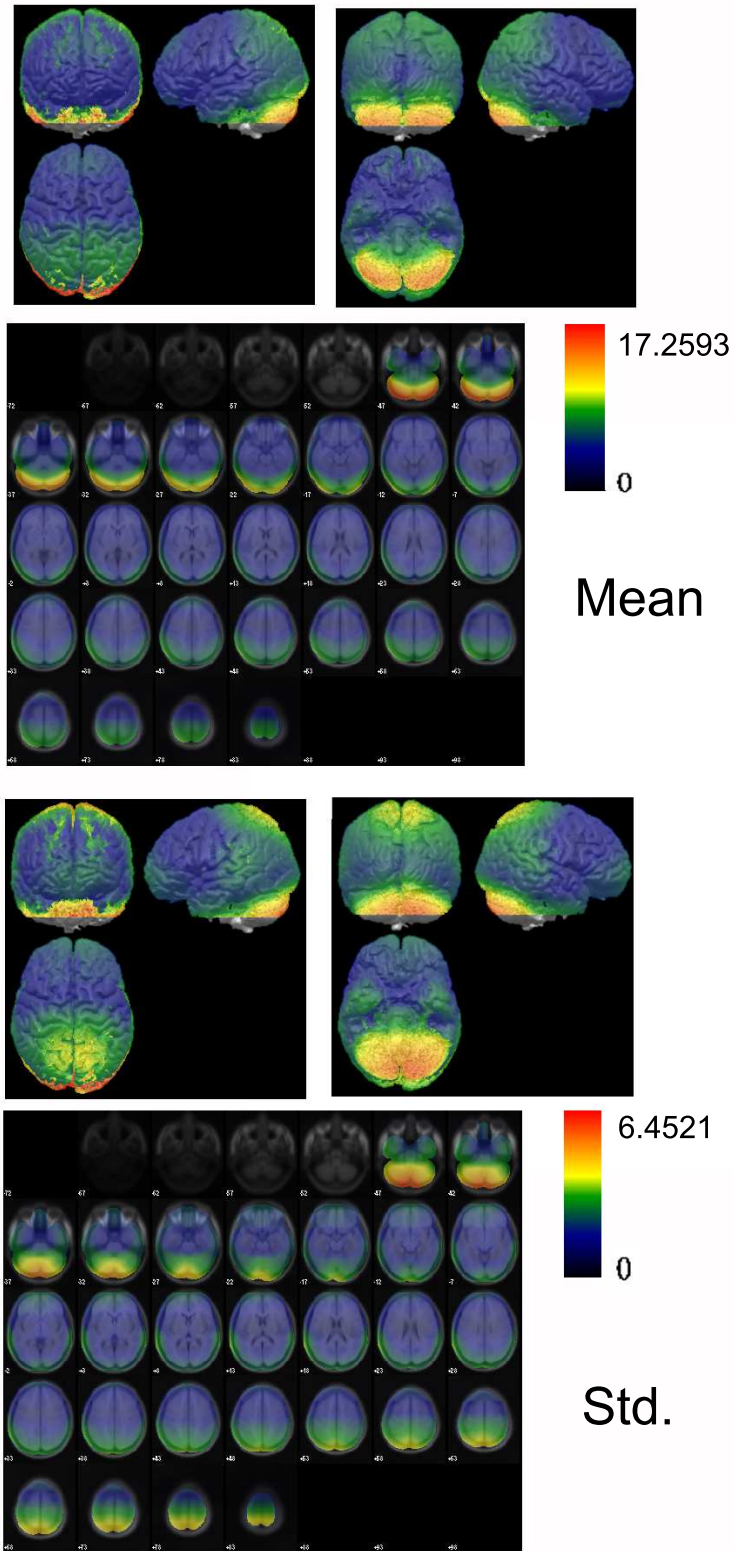
Figure 5.9: **Distribution of regional variation from Taiwanese subjects to MNI305.**
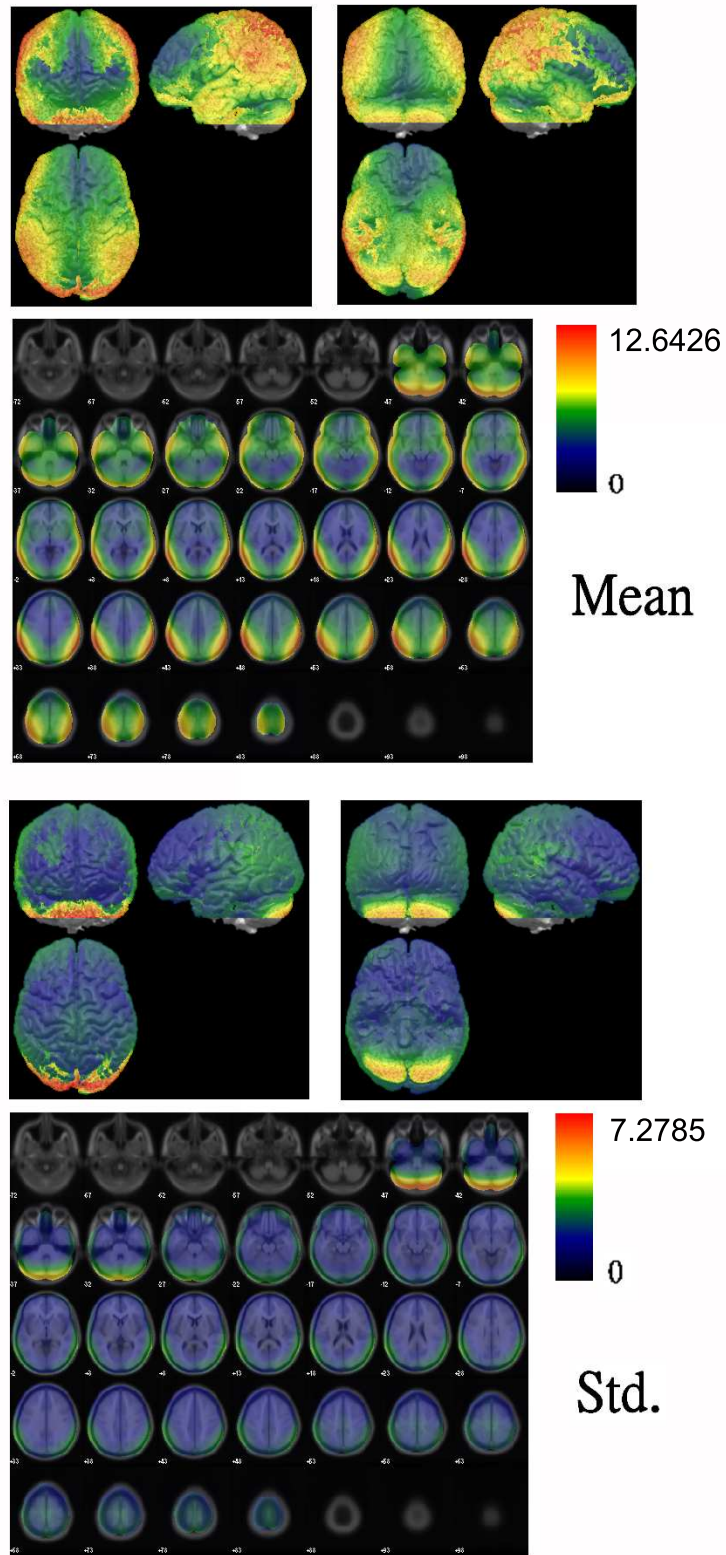
Figure 5.10: **Distribution of regional variation from Taiwanese subjects to ICBM152.**

5.2 Comparison of Different Gender Groups

In this section, difference between different gender groups would be revealed. The template construction procedure were also applied on the male and female population, 28 male and 30 female were jointed. For the observation result of Taiwanese gender templates accompanied with Korean gender templates, we may conjecture that head volume of male is larger than of female.

5.2.1 Ratio of Maximum Length and Maximum Width of Gender Templates

To compare the global characteristic of brain shape with different gender, we calculated ratio of maximum width to maximum length. Two measurements, maximum length and maximum width, were both defined on the slice that reveals AC-PC line as the middle line. The maximum length is the distance from the most anterior cortex to the most posterior cortex and the maximum width is the distance from the leftest cortex to the rightest cortex.

In figure 5.11 and table 5.9, we list brain ratio of Taiwanese male/female templates and Korean male/female templates. Data of Korean templates was referred to Lee et al. [23]. For a gender difference view, both gender templates of Korean and Taiwanese reveal that male templates are longer and wider than female templates, which implied head of male is larger than head of female. For an ethnic difference view, both of Taiwanese gender templates are a little shorter and wider than Korean gender templates.

5.2.2 Ratio of Gray Matter to White Matter

Table 5.10 lists gray-white matter ratio for gender groups. For Allen et al. [1]'s study, the gray-white matter ratio of women is 1.35 and 1.26 of men. For Gea et al. [9], they

	Templates			
	$Korean_M$	$Korean_M$	$Taiwanese_M$	$Taiwanese_F$
Length(cm)	16.5	15.6	16.32	14.892
Width(cm)	14.3	13.5	15.096	14.382
$\frac{Length}{Width}$	1.1538	1.1556	1.0811	1.0355

Table 5.9: **Ratio of maximum length and maximum width of gender templates.**
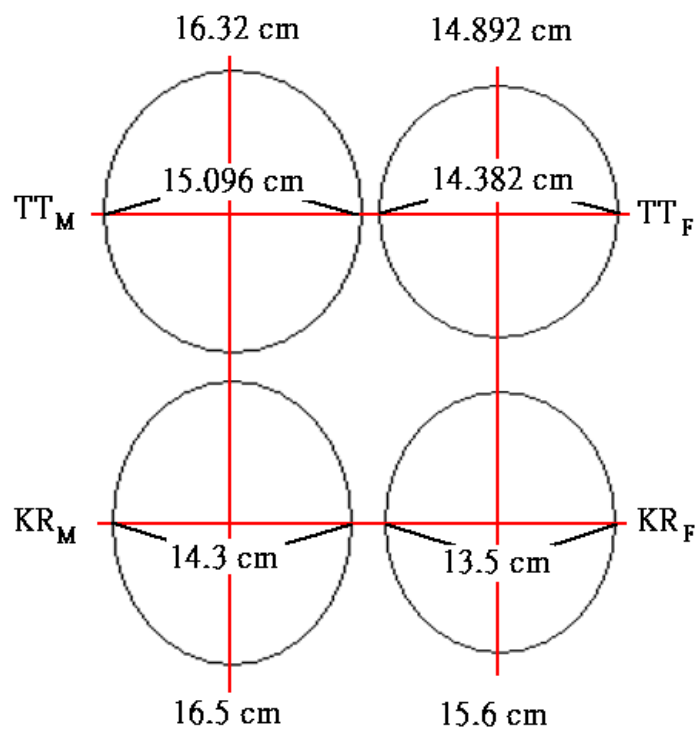
Figure 5.11: **Ratio of maximum length and maximum width of gender templates.** A measurement of global brain shape characteristic is to estimate the maximum length and maximum width of brain volumes. Here we defined the maximum length as the distance from the most anterior cortex to the most posterior cortex on the slice that reveals AC-PC line as the middle line. Besides, the maximum width was defined as the distance from the leftest cortex to the rightest cortex on the slice that reveals AC-PC line as the middle line.

claimed value of gray-white matter ratio for women is 1.4 and for men is 1.5. Our gray-white matter ratio for female is 1.5297 and for male is 1.4552. It seems there is no notable difference between gender groups.

Measurement	Taiwanese Subjects		Allen et al. [1]		Gea et al. [9]	
	Female	Male	Female	Male	Female	Male
Gray-White Ratio	1.5297	1.4552	1.35	1.26	1.4	1.5

Table 5.10: **Gray-white matter ratio of gender groups.**

Chapter 6

Conclusions

In this study, we have developed three methods, automatic mid-sagittal plane estimation method, representative brain determination method and 3D brain volume registration method, in order to construct a Taiwanese brain template. For brain registration, AC point, PC point and MSP were taken to be the mapping features. Therefore, the first step of our construction step was to automatically estimated MSP of every individual brain. The second step was to select a representative brain from these individual brains and then transformed representative brain's AC, PC to every individual brain. These transformed AC and PC were taken as the mapping features. Then, every individual brain would be scaled to the same size as the representative brain. Finally, all of these individual brains were averaged to form a Taiwanese brain template.

It is important to have a Taiwanese brain template for functional and structural researches. Brains for comparison need to be transformed to a standard coordinate for a reasonable comparison. A brain template could stand as a standard coordinate. By calculating the transformation between Talairach brain and Taiwanese brain template, the mapping between structural difference and its functional region could be found. In our study, we have demonstrated that a Taiwanese brain template could diminish the distortion of normalization, which also means to improve the accuracy of functional and structural mapping.

The observations from this study showed that Taiwanese brain template is shorter and wider than Western templates, including Talairach brain, MNI305, ICBM 152 and ICBM 452. This is the same result as Zilles et al. [43] and Kim et al. [18] proposed for Japanese and Korean population. Thus, we may conclude that the brains of Eastern people are roughly shorter and wider than the Western people.

Bibliography

[1] John S. Allen, Joel Bruss, and Hanna Damasio. The structure of the human brain: Precise studies of the size and shape of the brain have yielded fresh insights into neural development, differences between the sexes and human evolution. *American Scientist*, 92:246–253, 2004.

[2] B. Ardekani, J. Kershaw, M. Braun, and I. Kanno. Automatic detection of the mid-sagittal plane in 3D brain images. *IEEE Transactions on Medical Imaging*, 16(6): 947–952, 1997.

[3] K.S. Arun, T.S. Huang, and S.D. Blostein. Least-squares fitting of two 3D point sets. *IEEE Transactions on Pattern Analysis and Machine Intelligence*, 9(5):698–700, 1987.

[4] John Ashburner and Karl J. Friston. Nonlinear spatial normalization using basis functions. *Human Brain Mapping*, 7(4):254–266, 1999.

[5] L. G. Brown. A survey of image registration techniques. *Computing Surveys*, 24(4): 325–376, 1992.

[6] A.C. Evans, S. Marrett, P Neelin, L. Collins, K. Worsley, W. Dai, S. Milot, E. Meyer, and D. Bub. Anatomical mapping of functional activation in stereotactic coordinate space. *Neuroimage*, 1:43–53, 1992.

[7] A.C. Evans, D.L. Collins, S.R. Mills, E.D. Brown, R.L. Kelly, and T.M. Peters. 3D statistical neuroanatomical models from 305 MRI volumes. In *IEEE Nuclear Science Symposium and Medical Imaging Conference*, volume 3, pages 1813–1817, San Francisco, CA, USA, 1993.

[8] K.J. Friston, A.P. Holmes, K.J. Worsley, J.P. Poline, C.D. Frith, and R.S.J. Frackowiak. Statistical parametric maps in functional imaging : a general linear approach. *Human Brain Mapping*, 2:189–210, 1995.

[9] Yulin Gea, Robert I. Grossmana, James S. Babbc, Marcie L. Rabina, Lois J. Mannona, and Dennis L. Kolson. Age-related total gray matter and white matter changes in normal adult brain. part i: Volumetric mr imaging analysis. *American Society of Neuroradiology*, 23:1327–1333, 2002.

[10] H. Goldstein. *Classical Mechanics*. Addison-Wesley, 1950.

[11] T. Greitz, C. Bohm, S. Holte, and L. Eriksson. A computerized brain atlas: construction, anatomical content, and some applications. *Journal of Computer Assisted Tomography*, 15(1):23–38, 1991.

[12] G.J. Harris, P.E. Barta, L.W. Peng, S. Lee, P.D. Brettschneider, A. Shah, J.D. Henderer, T.E. Schlaepfer, and G.D. Pearlson. Mr volume segmentation of gray matter and white matter using manual thresholding: dependence on image brightness. *American Journal of Neuroradiology*, 15:225–230, 1994.

[13] P. Hellier, C. Barillot, I. Corouge, B. Gibaud, G. Le Goualher, D. L. Collins, A. Evans, G. Malandaln, N. Ayache, G. E. Christensen, and H. J. Johnson. Retrospective evaluation of intersubject brain registration. *IEEE Transactions on Medical Imaging*, 22 (9):1120–1130, 2003.

[14] C.J. Holmes, R. Hoge, L. Collins, R. Woods, A.W. Toga, and A.C. Evans. Enhance-

ment of MR images using registration for signal averaging. *Journal of computer assisted tomography*, 22(2):324–333, 1998.

[15] Q. Hu and W.L. Nowinski. A rapid algorithm for robust andautomatic extraction of the mid-sagittal plane of the human cerebrum from neuroimages based on local symmetry and outlier removal. *NeuroImage*, 20:2153–2165, 2003.

[16] D. V. Iosifescu, M. E. Shenton, S. K. Warfield, R. Kikinis, J. Dengler, F. A. Jolesz, and R. W. McCarley. An automated registration algorithm for measuring MRI subcortical brain structures. *Neuroimage*, 6(1):13–25, 1997.

[17] C. Izard, B. Jedynak, and C. Stark. Automatic landmarking of magnetic resonance brain images. *SPIE International Symposium on Medical Imaging*, February 2005.

[18] Hyun-Pil Kim, Jong-Min Lee, Dong Soo Lee, Bang-Bon Koo, Jae-Jin Kim, In Young Kim, and et al. Development of a group-specific average brain atlas : a comparison study between Korean and occidental groups. *Journal of Biomedical Engineering*, 26 (1):7–13, 2005.

[19] J. Kim and J.A. Fessler. Intensity-based image registration using robust correlation coefficients. *IEEE Transactions on Medical Imaging*, 23(11), 2004.

[20] J.H. Kim, J.M. Lee, U.C. Yoon, I.Y. Kim, J.S. Kwon, and S.I. Kim. Evaluation study of korean-specific tissue probability map with icbm tissue probability atlases: A probabilistic similarity index. In *10th International Conference on Functional Mapping of the Human Brain*, 2004.

[21] Peter J. Kostelec and Senthil Periaswamy. Image registration for MRI. *Modern Signal Processing*, 46:161–184, 2003.

[22] P.C. Lauterbur. Image formation by induced local interactions: Examples employing nuclear magnetic resonance. *Nature*, 242:190–191, 1973.

[23] J. S. Lee, D. S. Lee, J. Kim, Y. K. Kim, E. Kang, H. Kang, K. W. Kang, J. M. Lee, J. J. Kim, H. J. Park, J. S. Kwon, S. I. Kim, T. W. Yoo, K. H. Chang, and M. C. Lee. Development of Korean standard brain templates. *Journal of Korean medical science*, 20(3):483–488, Jun 2005.

[24] Y. Liu, R.T. Collins, and W. E. Rothfus. Automatic extraction of the central symmetry (mid-sagittal) plane from neuroradiology images. Technical Report CMU-RI-TR-96-40, Robotics Institute, Carnegie Mellon University, Pittsburgh, PA, November 1996.

[25] Y. Liu, R.T. Collins, and W.E. Rothfus. Robust midsagittal plane extraction from normal and pathological 3D neuroradiology images. *IEEE Transactions on Medical Imaging*, 20(3), 2001.

[26] J.B. Antoine Maintz and Max A. Viergever. A survey of medical image registration. *Medical Image Analysis*, 2(1):1–36, 1998.

[27] M. Mancas, B. Gosselin, and B. Macq. Fast and automatic tumoral area localization using symmetry. *Proceedings of the IEEE ICASSP Conference*, 2005.

[28] John Mazziotta, Arthur Toga, and et al. A probabilistic atlas and reference system for the human brain: International consortium for brain mapping (ICBM). *Philosophical Transactions of the Royal Society B: Biological Sciences*, 356(1412):1293–1322, 2001.

[29] J. Mykkänen, J. Tohka, J. Luoma, and U. Ruotsalainen. Automatic extraction of brain surface and mid-sagittal plane from PET images applying deformable models. Technical Report A-2003-1, Department of Computer and Information Sciences, University of Tampere, 2003.

[30] S. Prima, S. Oruselin, and N. Ayache. Computation of the mid-sagittal plane in 3D brain images. *IEEE Transactions on Medical Imaging*, 21(2):122–138, 2002.

[31] K. Sato, Y. Taki, H. Fukuda, and R. Kawashima. Neuroanatomical database of normal Japanese brains. *Neural Networks*, 16(9):1301–1310, 2003.

[32] K.A. Schaper, T.R. Jarvis, Kristi Boesen, Joseph Gati, Ravi Menon, and D.A. Rottenberg. Evaluation of brain grey-white ratios using automated tissue segmentation packages. 2005.

[33] T. Schormann, A. Dabringhaus, and K. Zilles. Statistics of deformations in histology and application to improved alignment with MRI. *IEEE Transactions on Medical Imaging*, 14(1):25–35, 1995.

[34] S.M. Smith. Fast robust automated brain extraction. *Human Brain Mapping*, 17(3): 143–155, 2002.

[35] Veronica Susanne Smith. *Evaluating Spatial Normalization Methods for the Human Brain*. PhD thesis, University of Washington, 2005.

[36] M.B. Stegmann, K. Skoglund, and C. Ryberg. Mid-sagittal plane and mid-sagittal surface optimization in brain MRI using a local symmetry measure. *SPIE International Symposium on Medical Imaging*, 5747, 2005.

[37] J. Talairach and P. Tournoux. *Co-Planar Stereotaxic Atlas of a Human Brain: 3-Dimensional Proprotional System V an Approach to Cerebral Imaging*. Thieme Medical Publishers, 1988.

[38] Leonid Teverovskiy and Yanxi Liu. Truly 3D midsagittal plane extraction for robust neuroimage registration. Technical Report CMU-RI-TR-04-21, Robotics Institute, Carnegie Mellon University, Pittsburgh, PA, March 2004.

[39] A.V. Tuzikov, O. Colliot, and I. Bloch. Brain symmetry plane computation in MR images using inertia axes and optimization. *Proceedings of the International Conference on Pattern Recognition*, 1:516–519, 2002.

[40] A.V. Tuzikov, O. Colliot, and I. Bloch. Evaluation of the symmetry plane in 3D MR brain images. *Pattern Recognition Letters*, 24(14):2219–2233, 2003.

[41] S. Umeyama. Least-squares estimation of transformation parameters between two point patterns. *IEEE Transactions on Pattern Analysis and Machine Intelligence*, 13 (4):376–380, 1991.

[42] P. Viola and W. M. Wells. Alignment by maximization of mutual information. *International Journal of Computer Vision*, 24(2):137–154, 1997.

[43] K. Zilles, R. Kawashima, A. Dabringhaus, H. Fukuda, and T. Schormann. Hemispheric shape of European and Japanese brains: 3D MRI analysis of intersubject variability, ethnical, and gender differences. *Neuroimage*, 13(2):262–271, 2001.

[44] Barbara Zitova and Jan Flusser. Image registration methods: a survey. *Image and Vision Computing*, 21(11):977–1000, 2003.